An ancient route towards salicylic acid and its implications for the perpetual *Trichormus–Azolla* symbiosis

Sophie de Vries[1]*, Cornelia Herrfurth[2,3], Fay-Wei Li[4,5], Ivo Feussner[2,3,6], Jan de Vries[7,8,9]

1 — Heinrich-Heine University Düsseldorf, Population Genetics, Universitätsstr. 1, 40225 Düsseldorf, Germany

2 — University of Goettingen, Albrecht-von-Haller-Institute for Plant Sciences, Department of Plant Biochemistry, Justus-von-Liebig Weg 11, 37077 Goettingen, Germany

3 — University of Goettingen, Goettingen Center for Molecular Biosciences (GZMB), Goettingen Metabolomics and Lipidomics Laboratory, Justus-von-Liebig Weg 11, 37077 Goettingen, Germany

4 — Boyce Thompson Institute, Ithaca, NY, USA.

5 — Plant Biology Section, Cornell University, Ithaca, NY, USA

6 — University of Goettingen, Goettingen Center for Molecular Biosciences (GZMB), Department of Plant Biochemistry, Justus-von-Liebig Weg 11, 37077 Goettingen, Germany

7 — University of Goettingen, Institute for Microbiology and Genetics, Department of Applied Bioinformatics, Goldschmidtstr. 1, 37077 Goettingen, Germany

8 — University of Goettingen, Goettingen Center for Molecular Biosciences (GZMB), Department of Applied Bioinformatics, Goldschmidtsr. 1, 37077 Goettingen, Germany

9 — University of Goettingen, Campus Institute Data Science (CIDAS), Goldschmidstr. 1, 37077 Goettingen, Germany

*Corresponding authors:

Sophie de Vries: rommels@hhu.de

Jan de Vries: devries.jan@uni-goettingen.de

ABSTRACT

Despite its small size, the water fern *Azolla* is a giant among plant symbioses. Within each of its leaflets, a specialized leaf cavity is home to a population of nitrogen-fixing cyanobacteria (cyanobionts). While examples of nitrogen fixing cyanobionts are found across the land plant tree of life, *Azolla* is unique in that its symbiosis is perpetual: the cyanobionts are inherited during sexual and vegetative propagation of the fern. What underpins the communication between the two partners? In angiosperms, the phytohormone salicylic acid (SA) is a well-known regulator of plant–microbe interactions. Using HPLC-MS/MS, we pinpoint the presence of SA in the fern; using comparative genomics and phylogenetics, we mined homologs of SA biosynthesis genes across Chloroplastida (Viridiplantae). While canonical isochorismate synthase (ICS) sequences are largely limited to angiosperms, homologs for the entire Phenylalanine ammonia-lyase (PAL)-dependent pathway likely existed in the last common ancestor of land plants. Indeed, *A. filiculoides* secondarily lost its ICS, but has the genetic competence to derive SA from benzoic acid. Global gene expression data from cyanobiont-containing and -free *A. filiculoides* unveil a putative feedback loop: SA appears to induce cyanobacterial proliferation, which in turn down-regulates genes in SA biosynthesis and its responses.

INTRODUCTION

The water fern *Azolla filiculoides* is best-known for its unique symbiosis with a nitrogen-fixing cyanobacteria, hereafter referred to as the cyanobionts (Rai et al., 2000). Unlike any other nitrogen-fixing symbiosis, the one of *Azolla* and its cyanobiont is vertically inherited from generation to generation (Peters and Meeks 1989, Zheng et al. 2009a, de Vries and de Vries 2018). Indeed, the cyanobiont cannot live without its host (Peters and Meeks 1989, Zheng et al. 2009b). This dependency is written in its genome, too (Ran et al. 2010): the genome has undergone a strong reduction and erosion. On the other side, when well-supplied with nitrogen nutrients *Azolla* is—in the lab—capable of living without its cyanobionts (Shi and Hall 1988). Yet, in nature the two partners occur together.

The *Azolla* cyanobiont is a section IV (Rippka et al. 1979), filamentous nitrogen-fixing cyanobacterium; taxonomically it is most commonly assigned to the genus *Anabaena* or *Nostoc*—but this affiliation is still debated (Pereira & Vasconcelos 2014; de Vries and de Vries 2018). As of late it is called *Trichormus azollae* (Pereira & Vasconcelos 2014). The cyanobiont lives in the leaf cavities of *Azolla* species (Peters and Meeks 1989) and co-occurs with several other bacterial associates, some which are denitrifiers, likely benefitting from the cyanobiont (Dijkhuizen et al. 2018). Additionally, some of the co-occurring bacteria appear to be inherited together with the cyanobiont (Zheng et al. 2009b).

The life cycle of *Azolla* is intertwined with that of its cyanobiont (Rai et al. 2000; Zheng et al. 2009a; de Vries and de Vries, 2018). During vegetative propagation (i.e. simple growth of the fern body and break-up into clonal “colonies”), cyanobiont populations are transferred to new leaf cavities via specialized trichomes (Calvert et al. 1985; Hill 1989). The trichomes grow out of the newly forming leaf cavities and get associated to the shoot apical meristem (Calvert and Peters 1981, Zheng et al. 2009b). On the apical meristem is a colony of hormogonia-like filaments of the cyanobiont (Peters et al. 1978, Peters and Meeks 1989); these filaments become attached to the branched trichome and as the leaf grows, both the trichome and the cyanobiont filaments are engulfed by the formed leaf cavity (Peters and Meeks 1989, Zheng et al. 2009a). Whether the other bacteria are transferred by the same means and whether as a result each leaf cavity is equipped with a highly similar microbiome is currently not known. During sexual propagation, the cyanobionts are attracted to the developing sporocarps, where they, similar to the vegetative propagation, become entangled in trichomes (Becking, 1987; Perkins and Peters 1993). While the formation of the indusium cell layer around the spores occurs, the cyanobionts are moved upwards to the tips of the

sporocarps, where they enter through the indusium pore into the forming indusium chamber (Perkins and Peters 1993). Upon maturation of the sporocarp, the cyanobionts in this chamber turn into resilient akinetes, facilitating the co-dormancy of symbiont and host (Perkins and Peters 1993, Zheng et al. 2009b). Hence, the process of sporocarp maturation and cyanobiont differentiation appears to be tightly coordinated (Zheng et al. 2009b). The molecular mechanisms that underpin this coordination are however unknown.

Vegetative propagation has been studied with regard to its chemical set-up. It appears that especially the trichomes are rich in phenolic compounds (Pereira & Carrapiço 2007). And it has been hypothesized that these phenolics may be relevant in some way for the transfer of cyanobionts from one cavity to another (Pereira & Carrapiço 2007). Indeed, it has been highlighted that the expression of a *chalcone synthase* (*CHS*) homolog of *A. filiculoides* is both responding to the absence of nitrogen and the absence of cyanobionts from the leaf pockets (Li et al. 2018, Eily et al. 2019). A recent study identified homologous genes encoding enzymes of the flavonoid biosynthesis pathway and functionally characterized a key enzyme, leucoanthocyanidin reductase (LAR) (Güngör et al. 2021). The identified homologs of the flavonoid biosynthetic genes (homologs of *chalcone isomerase* (*CHI*), *CHS* and *dihydroflavonol 4-reductase* (*DFR*) and *AfLAR*) appear co-expressed during the diurnal cycle of *A. filiculoides* independent of the nitrogen supply (Güngör et al. 2021). However, without nitrogen the genes rapidly decrease in expression level during the night cycle (Güngör et al. 2021).

Among the flavonoids that have been identified in *A. filiculoides* and also another water fern, *Azolla pinnata,* are derivatives of Caffeoylquinic acid, Dicaffeoylquinic (Epi-)Catechin, Quercitin and Kaempferol (Güngör et al. 2021). These flavonoids are involved in defense responses in other plants, e.g. the gymnosperms *Picea abies* (Danielsson et al. 2011). Similarly, another phenolic compound involved in plant defense, salicylic acid (SA) (Ding and Ding 2020), has also been implicated in altering the abundance of the cyanobionts and its expression of genes involved in nitrogen fixation (de Vries et al. 2018). This may suggest that a link between this highly coordinated symbiosis and the defense capabilities of *Azolla* has evolved in the 66-100mya old association (Hall and Swanson 1968, Collinson 2002; Carrapiço 2006).

SA can be synthesized via two distinct routes in land plants: In *Arabidopsis thaliana* the majority of SA stems from conversion of chorismate into isochorismate by isochorismate synthase (ICS) (Wildermuth et al. 2001, Garcion et al. 2008). Isochorismate is transferred from the chloroplast to the cytoplasm and as a substrate of avrPphB SUSCEPTIBLE3

(PBS3) conjugated with glutamate, resulting in the product isochorismate-9-glutamate (Rekhter et al. 2019). A spontaneous reaction, which can be also catalysed by ENHANCED PSEUDOMONAS SUSCEPTIBILTY 1 (EPS1), results in the conversion of isochorismate-9-glutamate to SA (Rekhter et al. 2019, Torrens-Spence et al. 2019). Yet, *EPS1* appears to be specific to Brassicaceae and a clear *PBS3* ortholog has not been identified in *A. filiculoides* (de Vries et al. 2018, Torrens-Spence et al. 2019, Li et al. 2020).

Already in other angiosperms than *A. thaliana*, SA may not come from the ICS-dependent pathway but rather derives from benzoic acid (Meulwy et al. 1995, Pallas et al. 1996, Coquoz et al. 1998). These early publications suggested that SA is synthesized via a Phenylaline Ammonia Lyase (PAL)-dependent pathway from phenylalanine. Phenylalanine is converted into *trans*-cinnamic acid (Widhalm and Dudareva 2015). From here, SA can be synthesized via peroxisomal β-oxidation or two cytoplasm-localized non-oxidative pathways, one CoA-dependent and one CoA-independent (Widhalm and Dudareva 2015). None of the pathways has so far full enzymatic evidence. Yet, some steps along the way have been functionally characterized. Some first importers of phenylpropanoid pathway-derived compounds into the peroxisome have been identified (Block et al., 2014). In the oxidative peroxisomal pathway, *trans*-cinnamic acid is converted into cinnamoyl-CoA (if the latter is not imported) via *trans*-cinnamic acid ligase (*Ph*-CNL) from *Petunia hybrida* and possibly also by its ortholog BENZOYLOXYGLUCOSINOLATE 1 (BZO1) in *A. thaliana* (Colquhoun et al. 2012, Klempien et al. 2012, Lee et al. 2012). In *P. hybrida* the following steps towards benzoyl-CoA are catalyzed via chalcone dehydrogenase (*Ph*CHD) and katalase1 (*Ph*KAT1) (Van Moerkercke et al. 2009, Qualley et al. 2012). In *A. thaliana* they are suggested to be realized by the multifunctional β-oxidation enzyme abnormal inflorescence meristem1 (*At*AIM1) and *At*KAT2 (Bussell et al. 2014, Widhalm and Dudareva 2015). The resulting benzoyl-CoA is converted to benzoic acid by a thioesterase, likely 1,4-dihydroxy-2-naphthoyl (DHNA)-CoA THIOESTERASE 1 (*At*DHNAT1/2) in *A. thaliana* (Widhalm et al. 2012, Widhalm and Dudareva 2015) or Ph-TE1 in *P. hybrida* (Adebesin et al. 2018). In the non-oxidative cytoplasmic pathways, a hydratase is suggested to use *trans*-cinnamic acid or cinnamoyl-CoA as a substrate and hydrates the double bond to form 3-hydroxy-3-phenylpropionic acid or 3-hydroxy-3-phenylpropanoyl-CoA, respectively (see Widhalm and Dudareva, 2015). Both of which are likely converted into benzaldehyde by a lyase-dependent reaction (see Widhalm and Dudareva, 2015). In *A. thaliana* benzaldehyde is converted to benzoic acid by Arabidopsis Aldehyde Oxidase4 (AAO4) (Ibdah et al. 2009), while in Snapdragon (*Antirrhinum majus*) it is imported into the mitochondrion and converted to benzoic acid by benzaldehyde dehydrogenase (BALDH) (Long et al. 2009). Independent

of the route benzoic acid is produced, it was suggested that benzoic acid 2-hydroxylase (BA2H)-like enzyme catalyzes the last step from there to SA (León et al. 1995).

In this study we explore the connections between SA and the coordinated symbiosis of the water fern *A. filiculoides* and its cyanobiont *T. azollae.* Using HPLC-MS/MS we measured SA in roots and the photosynthesizing sporophyte body of *A. filiculoides.* Because it is not known by which pathway the symbiotic system synthesizes SA, we used the cumulated knowledge on enzymatic synthesis of SA of the green lineage to identify candidate genes for SA biosynthesis in *A. filiculoides.* Applying comparative genomics and phylogenetics, we searched for orthologs—and the closest homologs—of key genes likely acting in the ICS- and PAL-dependent pathway; we further explored the possibility of cyanobiont-derived SA. We find that only the genomes of *Chara braunii, Selaginella moellendorffii* and angiosperms encode a separate standalone ICS. All other chlorophyte and streptophyte algae as well as bryophytes and the fern *Salvinia cucullata* contain a fusion enzyme, where the ICS domain is fused with a MenC and/or MenD domain, suggesting that chorismate can be quickly diverted into the phylloquinone pathway. Moreover, *A. filiculoides* entirely lacks an ICS-encoding gene. In contrast, our phylogenetic data support the presence of homologs for all known steps in the PAL-dependent pathway across land plants, suggesting that the benzoic acid pathway has the potential to be recruited for SA biosynthesis in several land plant lineages. Our data pinpoint the biosynthetic routes of SA via benzoic acid as the most likely origin of SA in *A. filiculoides.* We carried out global gene expression analyses on the *PAL*-dependent SA biosynthesis pathway and homologs to SA responsive genes. The majority of SA-associated genes that showed differential gene expression patterns appear to be down-regulated in the presence of the cyanobionts. Integrating this with previous results, we hypothesize that a feedback loop has co-evolved between the two partners, that tightly co-ordinates the levels of SA with the proliferation of the cyanobionts.

MATERIAL AND METHODS

Measurement of SA levels

The water fern *Azolla filiculoides* was cultured at 75% relative humidity in a heat-sterilized glass vessel. The ferns floated on 250 mL filtered water with a pH of 7.0. During the 16h-long day, the fern was exposed to 450 µmol quanta m^{-2} s^{-1} at 24 °C; during the 8h-long night, the temperature dropped to 20 °C. We picked plants from actively growing culture and used sterilized micro-scissors to separate the fern body into whole roots and green sporophyte tissue (i.e. with roots removed). Extraction was performed as previously described for lipids (Matyash et al., 2008), with some modifications specified previously (Iven et al., 2012). The

188 analysis was performed using an Agilent 1100 HPLC system (Agilent, Waldbronn, Germany)
189 coupled to an Applied Biosystems 3200 hybrid triple quadrupole/linear ion trap mass
190 spectrometer (MDS Sciex, Ontario, Canada) by using an ESI chip ion source (TriVersa
191 NanoMate; Advion BioSciences, Ithaca, NY, USA). The quantification of SA was performed
192 as previously described (Iven et al., 2012) applying a scheduled multiple reaction monitoring
193 detection in negative ionisation mode including the following MS transitions: 141/97
194 [declustering potential (DP) -45 V, entrance potential (EP) -7 V, collision energy (CE) -22 V]
195 for D_4-SA and 137/93 (DP -45 V, EP -7 V, CE -22 V) for SA. The quantification was carried
196 out using a calibration curve of intensity (*m/z*) ratios of [SA]/[D_4-SA] *vs.* molar amounts of
197 SA (0.3-1000 pmol).
198
199 Statistical analyses have been performed in R v.3.6.0. Data was tested for normality using a
200 Shapiro-Wilks test (Shapiro and Wilk, 1965), following a test to compare the variance of the
201 data between replicates of SA measurements from roots and sporophytes of *A. filiculoides*.
202 The data was normally distributed and showed no significant difference in variance.
203 Accordingly, a two-sample t-test (Student 1908) was computed.
204
205 **Identification and phylogenetic analyses of SA biosynthesis genes of *A. filiculoides***
206
207 For phylogenetic analyses, we worked with protein data from the genomes of *Anthoceros*
208 *agrestis* as well as *Anthoceros punctatus* (Li et al., 2020), *Amborella trichopoda* (*Amborella*
209 Genome Project, 2013), *Arabidopsis thaliana* (Lamesch et al., 2011), *Azolla filiculoides* (Li et
210 al., 2018), *Brachypodium distachyon* (The International Brachypodium Initiative, 2010),
211 *Capsella grandiflora* (Slotte et al., 2013), *Gnetum montanum* (Wan et al., 2018), *Marchantia*
212 *polymorpha* (Bowman et al., 2017), *Nicotiana tabacum* (Sierro et al., 2014), *Oryza sativa*
213 (Ouyang et al., 2007), *Picea abies* (Nystedt et al., 2013), *Physcomitrium patens* (Lang et al.,
214 2018), *Salvinia cucullata* (Li et al., 2018), *Selaginella moellendorffii* (Banks et al., 2011), and
215 *Theobroma cacao* (Argout et al., 2011); (b) the genomes of seven streptophyte algae:
216 *Chlorokybus atmophyticus* (Wang et al., 2020), *Chara braunii* (Nishiyama et al., 2018),
217 *Klebsormidium nitens* (Hori et al., 2014), *Mesotaenium endlicherianum* (Cheng et al., 2019),
218 *Mesostigma viride* (Wang et al., 2020), *Penium margaritaceum* (Jiao et al., 2020),
219 *Spirogloea muscicola* (Cheng et al., 2019). For each of the protein families, specific cutoffs
220 were chosen (see below). All sequences that have met the respective cutoffs, were aligned
221 using MAFFT v7.453 (Katoh and Standley, 2013) with the setting L-INS-I. Alignments were
222 cropped to conserved and alignable regions for all homologs. Maximum likelihood
223 phylogenies were computed using IQ-TREE multicore v.1.5.5 (Nguyen et al., 2015) with 100

bootstrap replicates. For finding the best model of protein evolution, we used ModelFinder (Kalyaanamoorthy et al., 2017). The best models were LG+G4 (Le and Gascuel, 2008) for PAL, LG+I+G4 for AIM1, KAT, LG+F+I+G4 for AAO, JTT+I+G4 (Jones et al., 1992) for DHNAT.

Protein sequences for enzymes involved in PAL-dependent biosynthesis of SA in *A. thaliana, P. hybrida* or Snapdragon (*Antirrhinum majus*) have been downloaded from TAIR (Lamesch et al., 2011), NCBI, and UniProt. Sequences have sampled by using an HMM search via HMMER 3.1b2 (Mistry et al., 2013) with the ammonia lyase domain (obtained from PFAM) as a query against the proteins from the above-described genomes; all sequences that met the inclusion threshold were retained. Additionally, HAL and fungal PAL sequences that were included in de Vries et al. (2017) were added. For computing the maximum likelihood phylogeny, we used only those sequences that were at least 600 amino acids in length.

For identification of putative ICS sequences in *A. filiculoides*, we conducted an HMM search using HMMER 3.1b2 (Mistry et al., 2013) for the chorismate binding domain against the high- and low-confidence protein sequences from the *A. filiculoides* genome v.1.1 (Li et al., 2018). We used all three thusly identified *Azolla* sequences that met the HMM search inclusion threshold (*e* values of $4.8*10^{-87}$, $4.6*10^{-85}$, and $3.7*10^{-84}$) as queries for a BLASTp search against the protein dataset from the above described genomes. To improve the sampling on the closest algal relatives of land plants, we additionally included sequences found via a tBLASTn in the transcriptomes of *Spirogyra pratensis* (de Vries et al., 2020), *Zygnema circumcarinatum* (de Vries et al., 2018), and *Coleochaete orbicularis* (Ju et al., 2015). We used only those sequences that have met an e value cutoff of 10^{-10}, had a minimum length of 300 amino acids.

Identification of SA biosynthesis genes in cyanobacteria

To identify the ICS of *T. azollae* we downloaded the ICS sequence of *Trichormus variabilis* from NCBI and used it in a BLASTp query against *T. azollae* in the non-redundant protein (nr) database of NCBI. To identify chorismate binding enzymes we blasted ICS, anthranilate synthase and aminodeoxychorismate synthase of *T. azollae* against cyanobacteria in the nr database. Further, we downloaded sequences for isochorismate pyruvate-lyase (IPL) from *Pseudomonas aeruginosa* (accession NP_252920.1) and salicylate synthase (SAS) of *Mycobacterium tuberculosis* (accession YP_177877.1). We used these sequences to identify IPL and SAS enzymes in cyanobacteria using BLASTp at NCBI.

Identification of homologs to SA responsive genes

We downloaded all protein sequences from TAIR10 (Lamesch et al. 2011) linked to the term response to SA. This resulted in 176 sequences, which we used as a query in a blastp search against the proteome of *A. filiculoides* (Li et al. 2018). The 16,776 non-unique hits were funneled into a reciprocal BLASTp search with max_target_seqs 1, returning the best hits from *A. thaliana* for 3,386 unique *A. filiculoides* proteins. We next retained only those sequences that had their best hit to one of the 176 accessions of *A. thaliana* associated with the term response to SA and used an e-value cutoff of 10^{-7}. The *A. filiculoides* sequences corresponding to the final list of hits against *A. thaliana* were considered homologs to SA responsive genes; and after removal of low-confidence proteins added up to 97 candidates.

Analyses of conserved sites in chorismate binding enzymes

Protein sequences of the chorismate binding enzymes of plants were separated into ICS, anthranilate synthase and aminodeoxychorismate synthase sequences according to the phylogenetic analysis. Further protein sequences of the top 100 blastp hits for each type of the cyanobacterial chorismate binding enzymes were downloaded from NCBI. Each subset of protein sequences was aligned with that of the anthranilate synthase of *Salmonella enterica* subsp. *enterica* serovar Typhimurium str. LT2 with MAFFT using a L-INS-I approach (Katoh and Standley, 2013) to identify the conserved positions described in Plach et al. (2015). To generate sequence logos for the respective groups the sequence from *Salmonella* was removed from the alignment after the positions were located. Sequence logos were generated based on the alignments.

Transcriptomic profiling of candidate genes for SA biosynthesis and signaling

Raw read count data for *A. filiculoides* with or without cyanobiont and treated with or without fixed nitrogen (NH_4NO_3) supply were obtained from Eily et al. (2019). We calculated the TPM for all datasets according to (Robinson and Oshlack, 2010) and used edgeR (Robinson et al., 2010) to calculate $\log_2$-foldchange and to identify the differently expressed genes (DEGs) within a given dataset. To calculate FDR from p-values a Benjamini-Hochberg correction was used.

Protein domain search

We used Interpro (Blum et al., 2020) to identify protein domains in chorismate binding enzymes of land plants and used the information of TIGR to identify the putative function of the chorismate binding enzymes identified in our BLASTp and phylogenetic analyses. Likewise, we used CD search (Marchler-Bauer et al., 2004) and the information of TIGR IDs

for protein domain analyses of cyanobacterial protein domains of chorismate binding enzymes.

RESULTS AND DISCUSSION

Azolla filiculoides produces SA

Molecular data on cross-talk and co-ordination between *Azolla* and its cyanobionts are just becoming more and more abundant (Brouwer et al. 2017, de Vries et al. 2018, Li et al. 2018, Eily et al. 2019, Güngör et al. 2020). Several studies point to a role of flavonoids in the communication between the two partners (Pereira and Carrapiço 2007, Güngör et al. 2020) and MeSA, a methylated, volatile derivative of SA, appears to also interfere in the interaction (de Vries et al. 2018). Yet, we do not know whether and how SA is synthesized endogenously in *A. filiculoides.*

In a first step, we measured endogenous SA levels in the roots and sporophyte of *A. filiculoides* (Table 1). The data confirmed that *A. filiculoides* harbors SA. Roots appear to harbor slightly more SA than the sporophyte (roots: 0.18±0.03 nmol/g fresh weight (FW), sporophyte: 0.09±0.02 nmol/g FW, p-value=0.0337). Yet, these basal levels of SA in the non-axenic *Azolla* are relatively low compared to for example Col-0 from *A. thaliana* (Rekhter et al. 2019). Regardless of how much SA was measured, the mere fact that it is present in the fern body begs the question of how it is synthesized. We thus next used the recently released genomic data on *Azolla filiculoides* to explore possible biosynthetic routes towards SA.

A treatise of the three possible routes for SA biosynthesis in *A. filiculoides*

Land plants have two biosynthetic routes towards SA. One route depends on ICS, the other on PAL (Vlot et al. 2009). Unlike other land plants, *Azolla* theoretically has a third option to acquire SA via the biochemical capacities of its omnipresent cyanobiont. Here we used a phylogenetic approach utilizing the genome data of *A. filiculoides* and a diversity of genomes from other species from the green lineage to identify putative candidates for the SA biosynthesis pathways in *Azolla*. We further investigated the cyanobiont genome with regard to its theoretical ability to synthesize the hormone.

The ICS-dependent pathway

The ICS-pathway is localized in the plastid and cytoplasm and requires ICS1 and 2 and PBS3 (Wildermuth et al. 2001, Garcion et al. 2008, Rekhter et al. 2019). The last step in the

conversion to SA can either be spontaneous or catalyzed by EPS1 (Rekhter et al. 2019, Torrens-Spence et al. 2019). EPS1 is Brassicaceae-specific (Torrens-Spence et al. 2019), but it is also not strictly required for the interaction. PBS3 has emerged from a lineage-specific expansion of GH3-encoding genes (de Vries et al. 2018, Li et al. 2020). However, two GH3-homologs exist in the *A. filiculoides* genome that fall into the same GH3 clade as *At*PBS3 (Li et al. 2018, Li et al. 2020 supplemental material). For the key enzyme, ICS, BLASTp surveys identified only a single low-confidence sequence in *A. filiculoides* (Li et al. 2018, 2020), which appears rather divergent to other ICS1 candidates as shown in the (supplemental) phylogenetic analyses included in Li et al. (2020). Here, we investigated the chorismate binding protein families in more detail.

Using an HMMsearch against the genome of *A. filiculioides,* we found three protein-coding genes (*Azfi_s0185.g056617*, *Azfi_s0002.g007267*, and *Azfi_s0061.g034905*) with a chorismate-binding domain (for which we obtained an HMM profile from PFAM; El-Gebali et al., 2019). ICS sequences exist throughout the green lineage, but we found no ortholog for *A. filiculoides* (Figure 1a). The existence of an ICS sequence in land plants and algae suggests that the last common ancestor of the Chloroplastida had an ICS sequence. The lack of an ICS in *A. filiculoides* can only be explained by a secondary loss; this absence is corroborated by the lack of clear ICS orthologs in the transcriptome data of *Azolla carolinia* (sequenced in the framework of the 1KP efforts; Carpenter et al., 2019) and *Azolla pinnata* (Shen et al., 2018; see supplemental Figure S1).

Whether the isochorismate pathway is used in all species with an ICS ortholog is however unclear when we investigated the protein domain structures of all ICS sequences. The ICS candidates from bryophytes, algae and the fern *S. cucullata* appear to be compound enzymes coupled with a MenC and/or MenD domain (Figure 1a). This suggests that in these species ICS may directly funnel isochorismate into the menaquinone pathway rather than into a route towards SA. Yet, in some of the species, such as the moss *Physcomitrium patens*, SA has been detected (Ponce De León et al., 2012). Thus, ICS was either recruited later in the evolution of land plants as the primary route towards SA or it is species specific whether SA derives from isochorismate or benzoic acid in plants. However, ICS may not be the only source for isochorismate.

Usually anthranilate synthases convert chorismate to aminodeoxyisochorismate and then to anthranilate. That said, a *Salmonella* anthranilate synthase was successfully engineered to become an isochorismate-forming enzyme by exchanging two amino acids in the active center (Plach et al. 2015). A mutation leading to a lysine at position 263 instead of glutamine

and another either at 364 changing a methionine to a lysine or at 365 changing lysine to valine led to isochorismate formation in *Salmonella* (Plach et al. 2015). These residues are more or less conserved across different phyla in bacteria (Plach et al. 2015): with Q263 and M364 being conserved across all analyzed anthranilate and aminodeoxychorismate synthases and L365 in the anthranilate synthases and I365 in the aminodeoxychorismate synthases. ICS and salicylate synthase (SAS) show a conserved K263, but appeared to be slightly more variable at positions 364 (ICS major amino acid (aa): 364L; SAS major aa: 364I) and position 365 (ICS major aa: 365V; SAS major aa: 365S). Further, the 263 lysine (K190 in *Escherichia coli*) was shown to be highly relevant for the function of bacterial ICS (Kolappan et al. 2007). We found that all land plant lineages included in this phylogeny, including *A. filiculoides*, also encode putative anthranilate synthases in their genomes (Figure 1a).

To elucidate whether the putative anthranilate synthases of Chloroplastida and of *A. filiucloides* in particular can potentially take over the role of ICS in the fern, we explored the respective positions determining the product specificity (a) in the set of land plant chorismate binding enzymes to establish the most abundant residues in land plants at these functionally relevant positions and (b) in the three *A. filiculoides* protein sequences. The anthranilate synthases of plants had the same aa pattern as bacterial anthranilate synthases: Q, M, and L (Figure 1b), while the aminodeoxychorismate synthases encoded mainly an E at the position equivalent to 263, and M, and I at the respective positions for 364 and 365 (Figure 1b). 263E was the second most abundant residue in aminodeoxychorismate synthases of bacteria (Plach et al. 2015), suggesting that the three residues are in general conserved across prokaryotes and eukaryotes. Plant ICS however showed a K, I and V at the respective positions in the alignment. All three positions were not variable in plant ICS (Figure 1b). This is corroborated by the fact, that the anthranilate synthase from *A. filiculoides* encoded a QML motif as any other land plant. Overall, this suggests that it does not fill in for the function of the missing ICS.

The PAL-dependent pathway

A PAL-dependent pathway for SA biosynthesis has been suggested for several angiosperms (Meuwly et al. 1995, Pallas et al. 1996, Coquoz et al. 1998). The synthesis of SA via PAL can be facilitated via several different routes of benzoic acid metabolism. All of them have in common that PAL, which converts phenylalanine to *trans*-cinnamic acid, is the entry point for SA synthesis (Widhalm and Dudareva, 2015). The β-oxidation pathway requires enzymes from the 4CL family and the closely related *At*BZO1/*Ph*-CNL clade, the hydratase *Ph*CHD, *Ph*KAT1and *At*DHNAT1/2 (Van Moerkercke et al., 2009, Colquhoun et al., 2012, Klempien

et al., 2012, Lee et al., 2012, Qualley et al., 2012, Widhalm et al., 2012, Widhalm and Dudareva, 2015). The non-oxidative pathway also requires 4CL, the hydratase AIM1, which is the ortholog of *A. thaliana* to *Ph*CHD, a lyase, AAO4 (Ibdah et al., 2009, Bussel et al., 2014, Widhalm and Dudareva, 2015) or in Snapdragon (*Antirrhinum majus*) the benzaldehyde dehydrogenase (BALDH; Long et al. 2009). The last step in the biosynthesis of SA is only indirectly characterized and an inhibitor study suggests that BA2H-like enzyme is required (León et al., 1995).

To identify PAL candidates in *A. filiculoides*, we performed an HMMsearch with the aromatic lyase motif (HMM profile obtained from PFAM; El-Gebali et al., 2019) against the genome of *A. filiculoides* as well as other representative species from across the streptophyte tree of life. The aromatic lyase motif is present in PAL, (P)TAL, TAM and PAL-tRNA synthase fusion proteins of plants. We used this dataset together with a subset of fungal PAL and eukaryotic HAL sequences (selected from the dataset of de Vries et al. 2017) to build a phylogeny.

In our phylogeny the fungal PAL, tRNA-PAL fusion proteins and eukaryotic HAL proteins each form their own clade (Figure 2). Yet, the functionally characterized PTAL and TAM sequences of plants fall into the midst of the putative PAL clade (Figure 2). A detailed study in *Sorghum bicolor* has identified two positions relevant for distinguishing PAL and PTAL (Jun et al. 2018): the presence of Phe at position 123 (relative to the characterized *Sb*PTAL Sb04g026510) and Lys at position 443, were present in sequences with PAL activity, while *Sb*PTALs showed His and Lys at the two respective positions. In *Os*TAM (Yan et al. 2015) these two positions are occupied by a Tyr and Asn respectively; the same combination of residues occurs in a *S. bicolor* PAL/PTAL candidate (Figure 2) that had neither tyrosine nor phenylalanine activity (Jun et al. 2018). To make more sense of the phylogenetic data, we mapped this sequence information of the two positions to the phylogeny.

While all HAL sequences occupied a 123S and 443M, the tRNA synthesis fusion proteins showed a deletion of both residues. In contrast, most sequences that fall into the plant and fungal PAL clade occupy Lys at position 443 (relative to Sb04g026510), with the exception of one very divergent sequence from *M. polymorpha* (Mapoly0142s0036.1.p; 443H) and the subclade including *Os*TAM (LOC_Os11g48110.1), which showed Asn at position 443 (Figure 2). Position 123 was more variant among fungal and plant PALs: Most fungal PALs have His at the relevant site, suggesting they may be PTALs instead. In contrast, most plant PAL candidates have a Phe at the site of interest, with the exception of the subclades including the monocot PTALs and TAM candidates and one *A. thaliana* PAL sequence

(123Y in *At*PAL3; Figure 2). In agreement, *At*PAL3 was found to have the lowest catalytic activity as phenylalanine ammonia lyase of all four PALs of *A. thaliana* (Cochrane et al. 2004). All seven included sequences of *A. filiculoides*, that were full-length and high-confidence sequences, showed a 123F and 443K (Figure 2), suggesting them as likely PAL candidates.

Next, we investigated the acyl-activating enzyme (AAE) family that includes *Ph*-CNL and its co-ortholog *At*BZO1 (Figure S2), and all *At*4CLs. Our analysis captured sequences from five of the seven predicted subfamilies of AAEs (Shockey et al., 2003). In general, we recovered four of the AAE subfamilies with a bootstrap support of at least 75. The family shows various lineage-specific expansions (Figure S2). Only AAE clade VII did not form a monophyletic clade (Figure S2). Clade I, IV, V and VI appear to have their origin in the last common ancestor of land plants, yet especially clade IV to VI show substantial lineage-specific radiation. Our enzymes of interest belong to these highly expanded clades: *At*BZO1 and *Ph*-CNL belong to AAE clade VI, and 4CL1,2,3 and 5 belong to AAE clade IV (Figure S2, Shockey et al., 2003). Despite that, we found four clear homologs of *A. filiculoides* for the 4CL-encoding genes (Azfi_s0003.g007625, Azfi_s0013.g013344, Azfi_s0114.g046013 and Azfi_s0030.g024259) and two candidates for AAE clade VI (BZO1/*Ph*-CNL; Azfi_s0159.g053935 and Azfi_s0002.g003721 [low-confidence sequence]). The next steps in the oxidative and non-oxidative pathways are catalyzed by hydratases *Ph*CHD in *P. hybrida* and likely by its ortholog *At*AIM1 in *A. thaliana* (Qualley et al. 2012, Bussell et al. 2014). Our phylogeny shows that an AIM1/CHD hydratase was present in the last common ancestor of Chloroplastida. While several lineages have species-specific expansions of the AIM1/CHD family, *A. filiculoides* possesses one clear ortholog for this hydratase (Azfi_s0256.g060521; Figure 3). A similar picture emerges for the next step in the peroxisomal pathway catalyzed by KAT: One KAT homolog was present in the last common ancestor of Chloroplastida, but KAT sequences have expanded in several lineages, most pronounced in the Brassicaceae (Figure 4). In contrast, the two sequenced fern genomes (*S. cucullata* and *A. filiculoides*), however, possess only one copy for KAT (Azfi_s0001.g000824, Figure 4). The final peroxisomal step to benzoic acid is realized by a thioesterase; *At*DHNAT1/2 shows activity on benzoyl-CoA esters (Widhalm et al. 2012) and was hypothesized for this step (Widhalm and Dudareva 2015). The DHNAT family more or less mirrors the species phylogeny, yet includes again species-specific radiations (Figure 5). In the ferns, we find a duplication for DHNAT homologs in *S. cucullata,* but one ortholog in *A. filiculoides* (Azfi_s0008.g011631; Figure 5).

In the non-oxidative pathway, two possible routes towards benzoic acid exist. Both start in the cytoplasm and require a hydratase (which is suggested to occur in both the cytosol and the peroxisomal pathway; and a lyase to synthesize benzaldehyde (Widhalm and Dudareva, 2015). The conversion from benzaldehyde to benzoic acid can occur via two different steps: (i) a cytoplasmic step, catalyzed by AAO4 in *A. thaliana* (Ibdah et al. 2009), or (ii) a mitochondria-localized step, as described for Snapdragon (*Antirrhinum majus*), where BALDH is converting the benzaldehyde to benzoic acid (Long et al. 2009). Given that for the last step towards benzoic acid different routes processed by distinct types of enzymes have been described, we analyzed both of them bioinformatically. Similar to the peroxisomal pathway, BALDH and AAO homologs must have already existed in the common ancestor of all Chloroplastida (Figure 6, S2). While algae contain only one homolog of BALDH, many of the land plant lineages show lineage-specific expansions on BALDH-like homologs (Figure S3). This also includes the fern *A. filiculoides.* In the ALDH2 clade that contains BALDH the fern *S. cucullata* has an ortholog*,* but not *A. filucloides* (Figure S3). That said, several sequences of *A. filiculoides* fall into the larger clade of ALDH1 and ALDH2 sequences, where they, however, only cluster with weak support (bootstrap value 61) with the ALDH1 rather than ALDH2 sequences. These are therefore the most likely candidates for a BALDH reaction (Azfi_s0021.g015740 [low-confidence sequence], Azfi_s0078.g038198, Azfi_s0049.g030778 and Azfi_s0083.g038897; Figure S3). As for the BALDH-like sequences, the AAO family shows lineage-specific radiation. This is most extensive in angiosperms and the lycophyte *S. moellendorffii* (Figure 6)*.* In contrast, the two ferns have each only one copy for AAO (for *A. filiculoides*: Azfi_s0158.g053886; Figure 6).

The PAL-dependent pathway is less-explored as a source for SA in land plants compared to ICS-dependent synthesis of SA. The PAL-dependent pathway, despite being highly radiated, has homologs for all enzymes being present at least in the last common ancestor of all streptophytes—going hand in hand with the idea that parts of this pathway were part of the genetic building blocks that allowed for the radiation of spezialized metabolism in land plants (Fürst-Jansen et al., 2020). This is most likely explained by the fact that this pathway is not a highly specialized pathway for SA biosynthesis, but instead recruits steps from other pathways, such as phenylpropanoid. With regard to the water fern *A. filiculoides,* our data adds more support to benzoic acid-derived SA than isochorismate-derived SA biosynthesis (Figure 7). In this unique system, however, another plausible route for synthesizing SA exists. Cyanobacteria from the Nostocaceae, to which the cyanobiont belongs, can synthesize SA (Toribio et al. 2020) and it is possible that *A. filiculoides* has an alternative reservoir for this phytohormone.

The cyanobionts' pathway

Instead of producing SA autonomously, it is theoretically conceivable that the cyanobiont produces SA *for A. filiculoides.* We therefore investigated the cyanobionts genome for its genetic capability to synthesize SA. Bacteria produce SA either via ICS and IPL enzymes or directly via salicylate synthase (Ankenbauer and Cox, 1988, Gaille et al., 2002, Zwahlen et al., 2007). Indeed, in several Nostocaceae SA has been measured (Toribio et al. 2020). This leaves the possibility that between *Azolla* and its cyanobiont a tight regulation of SA-derived host responses has co-evolved.

We searched for ICS sequences in *T. azollae* using the ICS sequence from *T. variabilis*; we retrieved three sequences annotated as ICS (WP_013190659.1; query coverage 97%, % identity 68.63%, e-value 0), anthranilate synthase component I (WP_013192196.1; query coverage 63%, % identity 27.48%, e-value $2*10^{-23}$) and aminodeoxychorismate synthase component I (WP_013189914.1; query coverage 71%, % identity 27.54%, e-value $1*10^{-28}$; Figure 8a). Isochorismate is converted to salicylic acid via IPL (Gaille et al., 2002). Therefore, we next searched for an IPL candidate in *T. azollae.* Using the functionally characterized IPL of *Pseudomonas aeruginosa* (Gaille et al., 2002) as a query for a BLASTp, we found no hits in the genome of *T. azollae* but in several other cyanobacteria, including the order Nostocales and the family Nostocaceae, to which *T. azollae* belongs (Figure 8b). Thus, while some *Nostoc* species are able to synthesize SA (Toribio et al. 2020), only three different species from the Nostocaceae encoded an IPL sequence (Figure 8b).

Some bacteria use salicylate synthase, which directly converts chorismate to SA. Therefore, we queried the functionally characterized salicylate synthase from *Mycobacterium tuberculosis* (Zwahlen et al. 2007) in a BLASTp search against (a) *T. azollae* (supplemental data S1A) and (b) all cyanobacteria (supplemental data S1B). In the search against *T. azollae* we retrieved two hits; one against anthranilate synthase component I (e-value $6*10^{-28}$), of which the best hit in a protein domain search was indeed against anthranilate synthase component I (TIGR00564, e-value 0) and one against ICS (e-value $2*10^{-18}$), but no hit to an annotated salicylate synthase. In contrast to the IPL distribution, the most hits of salicylate synthase were in the family of Nostocaceae (Figure 8c). All of the top100 salicylate synthase-like sequence from diverse cyanobacteria, were predicted to contain a salicylate synthase domain (TIGR03494). Yet, all sequences also matched TIGR domain annotations for an ICS domain (TIGR00543), an aminodeoxychorismate synthase component I domain (TIGR00553) and an anthranilate synthase component I domain (TIGR00564). The positions

554 for all domain annotations were partially overlapping. This is in contrast to the two
555 sequences retrieved for *T. azollae,* which had their best TIGR domain hits to an anthranilate
556 synthase component I (TIGR00564, e-value 0) and ICS domain (TIGR00543, e-value
557 $4.75*10^{-107}$).
558
559 As described above engineered anthranilate synthases from *Salmonella* had been described
560 to convert chorismate to isochorismate instead of anthranilate (Plach et al. 2015). Some of
561 these anthranilate synthase mutants even directly synthesized SA from chorismate (Plach et
562 al. 2015). We, thus, had a closer look at the putative chorismate binding enzymes of *T.*
563 *azollae*. Similar to our analyses for the anthranilate synthase of the host, we aligned the
564 protein sequences of *T. azollae* with that of the anthranilate synthase from *S. enterica*
565 subsp. enterica serovar Typhimurium str. LT2. As described for several major phyla of
566 bacteria (Plach et al., 2015), the anthranilate synthases of cyanobacteria had the QML motif,
567 and the cyanobacterial aminodeoxychorismate synthases encoded the expected QMI motif
568 (Figure 8d). Likewise, salicylate synthase and ICS encoded usual motifs with KLS and KLV,
569 respectively (Figure 8d).
570
571 Cyanobacterial anthranilate synthase, including that of *T. azollae,* and
572 aminodeoxychorismate synthase have the QML and QMI motif. Hence, they show the typical
573 aa pattern for these types of enzymes (Plach et al. 2015) and are likely not involved in SA
574 biosynthesis. The ICS had a KLV motif, frequently found for bacterial ICS sequences (Plach
575 et al. 2015). This suggests that *T. azollae* is capable of synthesizing isochorismate but not
576 SA. Given that *Trichormus* species have been shown to produce SA (Toribio et al. 2020), it
577 can be envisioned that *T. azollae* lost its salicylate synthase or IPL. Indeed, during the 66-
578 100 million years of co-evolution between fern and cyanobiont (Hall and Swanson 1968,
579 Collinson 2002; Carrapiço 2006), the genome has started to erode, evident by a high
580 proportion of pseudogenes (Ran et al. 2010). It could therefore, be that due to SA being
581 synthesized by *Azolla, T. azollae* lost its SA synthesizing capabilities. Isochorismate in
582 bacteria can be funneled into the menaquinone pathway (Daruwala et al. 1996, Meganathan
583 and Kwon 2009) or to produce SA under iron deficiency, possibly to act as a siderophore
584 (Visca et al. 1993). In the here described scenario isochorismate of the cyanobiont would
585 singularly be used for menaquinone biosynthesis, while potential SA-associated
586 siderophores may require SA from *Azolla* to be shuffled to its symbiont. However,
587 isochorismate can decompose at slow rates directly into SA and the existence of an IPL may
588 not be necessary when the other isochorismate-metabolizing route towards menaquinone is
589 not active (Rekhter et al. 2019).
590

PAL-dependent routes appear the most likely path towards SA in Azolla

All major land plant lineages and green algae appear to encode an ICS sequence in their genomes (Figure 1a). This includes the only other sequenced fern genome of *Salvinia cucullata*—but not that of *A. filiculoides*. This warrants attention. If we rule out simple technical errors, *A. filiculoides* appears to have secondarily lost its ICS sequence and by that its ability to synthesize isochorismate. It is conceivable that during the evolutionary history of plants and algae, SA biosynthesis had already once been recruited from a cyanobiont—the cyanobacterial plastid progenitor (Gross et al., 2006). In the Brassicaceae *A. thaliana* ICS is localized to the plastid, where it synthesizes isochorismate (Wildermuth et al. 2001, Garcion et al. 2008), which is then transferred to the cytoplasm to be further processed into SA (Rekhter et al. 2019). It is thus tempting to speculate that this is a case where the tape of evolution is replayed: the fern *Azolla* receives isochorismate from its symbiont, *T. azollae*, and uses this backbone molecule to synthesize SA. Indeed, the genome of *T. azollae* shows clear traces of an obligate symbiont and—based on its genome structure and its mode of inheritance—was speculated to be an organelle in the making (Ran et al. 2010). Yet no cases of endosymbiotic gene transfer have been reported for the genome of *A. filiculoides* (Li et al. 2018). Indeed, cyanobiont-free *Azolla* species can survive with ample nitrogen supply (Brouwer et al., 2017). Thus, while it is a fascinating area of speculation, we would suggest that *Azolla* does not have to rely on the cyanobionts for the synthesis of its defense hormone.

Overall, it appears to be more likely that *Azolla* uses the PAL-dependent pathway. This does not exclude that *T. azollae* requires host-derived SA. Indeed, that both partners rely on the phytohormone to some degree is in agreement with our previous data, where exogenous application of an SA-derivative triggered alterations in host and cyanobiont gene expression patterns as well as cyanobiont abundance (de Vries et al. 2018). The obvious question following this is, whether SA biosynthesis and SA response can be modulated by the cyanobionts. To gain first insights, we next investigated the expression profile and differential gene expression (DGE) of the PAL-dependent biosynthesis pathway and SA responses of *A. filiculoides* upon changes in nitrogen availability and presence/absence of the cyanobiont.

Alterations in the cyanobionts population influence the gene expression patterns for benzoic acid-derived SA biosynthesis

Nitrogen availability has been shown to modulate expression of genes involved in the synthesis of phenylpropanoid-derived flavonoids in *A. filiculoides* (Güngör et al. 2021). Indeed, the absence of cyanobionts also change expression levels of *CHS* in *A. filiculoides*

(Eily et al. 2019), overall linking the phenylpropanoid-derived compounds to the symbiosis. SA, which is a conceivable phenylpropanoid-derived compound in *A. filiculoides*, is also a regulator of flavonoids (Nugroho et al. 2002, Tounekti et al. 2013, Ni et al. 2018). In bacteria, SA is likely used as a siderophore to sequester iron from iron-poor environments (Visca et al. 1993). Furthermore, in 2018 we have shown that SA can influence the population size of the cyanobionts and their nitrogen fixation-related gene expression (de Vries et al., 2018). To explore these factors, we (a) investigated the gene expression profiles upon these two factors and (b) calculated the DGE for *A. filiculoides* with resepct to the PAL-dependent pathway.

To understand the global gene expression patterns of genes for SA synthesis and down-stream pathways in *A. filiculoides*, we first analyzed gene expression levels in Transcript Per Million (TPM, supplemental data S2A and S3A). In total, we investigated 19 high-confidence candidate genes; 18 of these showed an average TPM above 1 in at least one condition. *A. filiculoides* invested a pronounced transcript budget into the phenylpropanoid pathway: while the cumulated expression of all genes amounted to an average (over all conditions) of 2734.79±544.91 TPM, the 11 homologs of genes from the canonical phenylpropanoid pathway (7 *PAL*-, and 4 *4CL*-homologs) made up 2335.55±535.27 TPM—which was largely due to the PAL homologs. Of the seven putative PAL-coding genes, one distinguished itself (*Azfi_s0123.g048412*) by dwarfing all the other average gene expression levels with a TPM of 1757.05±338.51. At the same time, *Azfi_s0123.g048412* had the most stable expression level, never showing differential gene expression changes under the conditions analyzed here. For comparison, the TPM of 4CL amounted to 24.44±11.58.

11 of 19 high-confidence candidate genes for the SA biosynthesis pathway in *A. filiculoides* showed significant changes in their differential gene expression patterns due to supply of fixed nitrogen and/or presence of the cyanobiont (Benjamini Hochberg adjusted FDR ≤ 0.05; Figure 9a based on the pathways shown in Figure 7, Supplemental data S2B); 8 of these 11 genes were up or down-regulated with a $\log_2$(fold-change[FC]) > 1 or <-1. The absence of fixed nitrogen alone in presence of the cyanobiont (nYcY vs. nNcY) or the absence of the cyanobiont in presence of fixed nitrogen (nYcY vs. nYcN) has only a small effect on the expression of the PAL-dependent biosynthesis pathway: only 3 of 19 genes showed differential gene expression in either of the comparisons. Most changes were observed when comparing the presence of cyanobionts (nNcY) to the absence of cyanobionts (nNcN) in the absence of fixed nitrogen (8/19 differentially expressed genes) and when comparing presence of fixed nitrogen and cyanobiont (nYcY) with the absence of both (nNcN; 9/19 differentially expressed genes). These two comparisons shared seven differentially

665 expressed genes, of which two (belonging to gene families *PAL* and *BALDH*) were up and
666 five were down-regulated (belonging to gene families *PAL, 4CL, BALDH* and *AAO4*) in both
667 conditions.
668
669 The two initial steps in the core phenylpropanoid pathway, *PAL* and *4CL*, the initial step in
670 the β-oxidative pathway (*BZO1*) and the last steps in the conversion of cytoplasmic
671 benzaldehyde to benzoic acid (*AAO4* and *BALDH*) were responsive on a gene regulatory
672 level (Figure 9a). The peroxisomal steps catalyzed by gene families *AIM1, DHNAT1/2* and
673 *KAT* showed little differential gene expression; only the *AfKAT* candidate was minimally
674 induced (log_2(FC)=0.38; FDR=0.02) when both nitrogen and cyanobiont conditions were
675 changed (nYcN vs. nNcY). This is in agreement with the phenylpropanoid pathway being
676 regulated on a transcriptional level (e.g. Weisshaar and Jenkins 1998, Deluc et al. 2006, Xie
677 et al. 2008). *PAL* genes are responsive to biotic stressors (Oliva et al. 2015, Reboledo et al.
678 2021). It is therefore, in general, not surprising that genes from the phenylpropanoid
679 pathway are responsive to the treatment. In addition, the late steps in the pathway are
680 modulated due to the availability of the cyanobiont and fixed nitrogen. Hence not only SA
681 appears to alter the abundance of the cyanobiont and expression of genes relevant for
682 nitrogen fixation (de Vries et al. 2018), availability of both components also influences SA
683 biosynthesis. This suggests an intricate system of communication between the two partners.
684
685 The pattern of how SA biosynthesis is regulated on the gene level appears complex.
686 Sometimes it is contrasting within a gene family or opposite responses occur when changes
687 in cyanobiont presence/absence is evaluated compared to when changes in the availability
688 of fixed nitrogen are evaluated. It appears that in the presence of cyanobionts more genes
689 are down-regulated than up-regulated, though (Figure 9a). Assuming that down-regulation of
690 genes in the SA biosynthesis pathway translates into less SA being produced, this appears
691 to be in contrast with SA levels being induced during colonization of some symbionts in other
692 plants (Fernández et al. 2014). However, it was noted that such defenses are early on
693 responses, hypothesized to stop symbionts from too much proliferation (Plett and Martin
694 2018). An integrated symbiont, however, is a long-term association. Thus, using SA to limit
695 proliferation within a host early on during symbiosis is not relevant. Moreover, in our
696 previous data on exogenous application of MeSA, we observed an increase of the
697 cyanobiont after treatment (de Vries et al. 2018). Taken together with the expression data on
698 the putative SA biosynthesis genes one may hypothesize a feedback loop between the
699 accumulation of SA and the accumulation of the cyanobiont. This is in agreement with MeSA
700 reducing the expression of the gene encoding iron-dependent niFE (de Vries et al. 2018).
701

Expression profile of SA responsive pathways in *A. filiculoides* show distinct responses towards the availability of fixed nitrogen and the cyanobiont

In several land plant species, SA levels are induced during interactions with beneficial microbes (Blilou et al. 1999, Blilou et al. 2000, Liu et al. 2003, Pozo et al. 2015). Further cyanobacterial treatment of *A. thaliana* resulted in the induction of SA controlled gene expression (Belton et al. 2020). Above, we showed that gene expression levels associated with SA biosynthesis are reduced in presence of the cyanobionts. Hence, we wondered whether SA responsive genes may also differ in their gene expression in this particular symbiosis compared to less intimate ones.

We downloaded all *A. thaliana* protein sequences of genes that are associated with the term 'SA responses' from TAIR (Lamesch et al., 2011). These 176 sequences were used as a query in a reciprocal BLASTp approach, first against all proteins of *A. filiculoides* and the thusly obtained homologs back against *A. thaliana*. In total we found 105 homologs, of which 97 are high confidence proteins. These 97 homologs correspond to 47 different SA-responsive proteins of *A. thaliana* involved in various processes (Figure 9b, Supplemental data S3B). Overall, 55.7% of the homologs of SA-responsive genes show differential gene expression (FDR<0.05) in at least one comparison. Similar to the SA biosynthesis expression, SA-derived responses showed most differential expressed genes in the comparisons nNcY vs. nNcN (31/97 homologs) and nYcY vs. nNcN (35/97 homologs). Of those genes, 23 were shared between the conditions, nine were up-regulated and 14 down-regulated (FDR<0.05). Corroborating the results of the expression patterns of the SA biosynthesis, changes in the availability of fixed nitrogen have only little influence on the expression of SA responsive genes. Independent of the presence of the cyanobiont only two (nYcY vs. nNcY) and seven genes (nYcN vs. nNcN) were significantly changed in their expression (FDR <0.05). Of those only one (*Azfi_s0427.g069291*) showed the same direction of regulation, and was induced in both treatments (log_2-foldchange=1.64 in nYcY vs. nNcY and log_2-foldchange=2.31 in nYcN vs. nNcN). *Azfi_s0427.g069291* was also induced in comparisons where presence of fixed nitrogen and cyanobiont was changed (FDR<0.05). *Azfi_s0427.g069291* encodes a putative 2-oxoglutarate (2OG)/Fe(II)-dependent oxygenase (2-ODD) superfamily protein. Given the diversity of reactions in specialized metabolism and hormone homeodynamics that are catalyzed by 2-ODDs it is difficult to make an educated prediction of what the regulation of this 2-ODD means. That said, it is an interesting candidate enzyme for future studies.

Overall, presence of nitrogen compared to its absence and presence of the cyanobiont compared to its absence result in more genes associated with a response to SA being

down-regulated than up-regulated (Figure 9b). This indicates that SA signaling is reduced in the presence of fixed nitrogen. The observation was more pronounced when the presence of the cyanobiont was altered than when the availability of fixed nitrogen was changed. This is due to the generally low transcriptional response to changes in fixed nitrogen. In contrast to the abundance of down-regulated genes in response to a change of one component in the system, changes in both components lead to a complex dysregulation of putative SA-responsive genes (Figure 9b).

Many of the differentially expressed genes are found in the category of transcription factors and MAP kinases. Here most homologs appear down-regulated when the presence of the cyanobiont is compared to its absence, independent of the availability of nitrogen (FDR <0.05, Figure 9b). In the comparison of nYcY vs. nYcN eight *TFs* are down-regulated and only three are up-regulated. Also, two *MAP kinase* homologs are down-regulated and none are up-regulated. In nNcY vs. nNcN 10 *TFs* and four *MAP kinases* show down-regulation, while five *TFs* and no *MAP kinase* show up-regulation. It appears that especially up-stream regulators of defense responses are affected by the presence of the cyanobiont. This is in agreement with the reduction of gene expression of the putative SA biosynthesis pathway we observed in the same comparisons (Figure 9a). In contrast, SA signaling was induced upon treatment of *A. thaliana* with *Nostoc punctiforme* PCC 73102 (Belton et al. 2020), a cyanobacterium from the same family as *Azolla*'s cyanobiont. *N. punctiforme* PCC 73102 is a strain with symbiotic competence that is often used in experiments with cyanobacteria and different hosts (Meeks et al. 2001, Warshan et al. 2017). This fits the hypothesis of Plett and Martin (2018), that early increase in SA during symbioses may be to establish the borders of same associations. However, the association between *T. azollae* and the water fern is perpetual. It is thus to be expected that the usual early responses to encountering potential symbionts are not mirrored in this vertically inherited association. Besides, data on host-symbiont interaction is often gathered from angiosperm systems. Data related to SA signaling in other plants during interaction with pathogenic microorganisms already indicate differences in the defense network; for example, the antagonism between SA and another phytohormone, jasmonic acid, appears to not exist in spruce during infection with a necrotrophic pathogen (Arnerup et al. 2013). Additionally, it appears that the genes coding for the Arabidopsis SA receptors *At*NPR1, 3 and 4, which have contrasting roles in SA signaling (Ding et al. 2018), arose from a lineage-specific radiation (Li et al. 2020, supplemental data therein). In *A. filiculoides* two possible candidates for *NPR* homologs, likely derived from a lineage-specific duplication, are found (Li et al. 2020, supplemental data therein). Euphyllophytes thus likely had only a single ancestral NPR protein. Given these

775 data, it is reasonable to assume that SA signaling is in *A. filiculoides* in general and in the
776 symbiosis of the fern only partially similar to that of model angiosperms.
777
778 **Conclusion**
779 The phytohormone SA is important for biotic interactions in plants and iron-sequestration in
780 bacteria. Previously, we showed that SA is a candidate molecule involved in the tight
781 coordination of the symbiosis between *A. filiculoides* and its cyanobionts (de Vries et al.,
782 2018). Here, we investigated the possible routes by which SA may be synthesized in
783 *A. filiculoides* as well as how the cyanobiont and the availability of fixed nitrogen influence
784 gene expression patterns that can be associated with SA biosynthesis and signaling. Our
785 data pinpoint that the most likely biosynthetic route towards SA in the fern derives from
786 benzoic acid, rather than isochorismate. Although the cyanobiont is genetically capable of
787 synthesizing the latter, it lacks genes encoding IPL or salicylate synthase to convert
788 isochorismate or chorismate to SA. Most genes relevant for SA biosynthesis in the water
789 fern as well as homologs to genes associated with response to SA are down-regulated in *A.*
790 *filiculoides* with a cyanobiont compared to a *Trichormus*-free culture. Most of the differential
791 regulation appears to be on up-stream regulators such as *TFs* and *MAP kinases.* Taken our
792 previous and new data together, SA might participate in a feedback loop between *A.*
793 *filiculoides* and *T. azollae*.
794
795 **ACKNOWLEDGEMENTS**
796 JdV thanks the European Research Council for funding under the European Union's Horizon
797 2020 research and innovation programme (Grant Agreement No. 852725; ERC-StG
798 "TerreStriAL"). IF gratefully acknowledges support by the Deutsche
799 Forschungsgemeinschaft (INST 186/822-1).
800
801 **TABLE**
802
803 **Table 1. Quantification of salicylic acid (SA) in root and green sporophyte tissues of**
804 ***Azolla filiculoides* via HPLC-MS/MS.**

tissue type	biological replicate	weight f.w. [g]	SA [nmol/g f.w.]
whole root	I	0.02	0.22
	II	0.01	0.17
	III	0.025	0.14
sporophyte	I	0.105	0.1
	II	0.1	0.11
	III	0.11	0.07

805 Abbreviations: f.w. = fresh weight

FIGURE LEGENDS

Figure 1. Evolution of chorismate binding enzymes in the green lineage. (a) ML-phylogeny of chorismate binding enzymes from Chloroplastida with 100 bootstrap replicates. Sequences from *A. thaliana* are highlighted in pink and sequences of *A. filiculoides* are highlighted in blue. We recovered three clear clades, one for isochorismate synthases (ICS), one for aminodeoxychorismate synthases and *p*-aminobenzoate synthases and one for anthranilate synthases. Bootstrap support of 100 is indicated by black dots on the branches. On the right we indicate TIGR domain annotations for the for different categories of chorismate binding enzymes. Black dots indicate which domain was found; no dot indicates that no TIGR domain annotation was present for this sequence. White dots only occur for collapsed branches, to indicate for which of the collapsed sequences a domain annotation was available (black dot) and for which not (white dot). (b) Conserved sequence logos for the clades containing anthranilate synthase, aminodeoxychorismate/*p*-aminobenzoate synthase and isochorismate synthase (ICS) shown in (a). Highlighted residues correspond to amino acids that have been suggested to be functionally relevant for the product specificity of these enzyme categories in Plach et al. (2015).

Figure 2. Phylogeny of PAL and HAL sequences from eukaryotes and prokaryotes. ML-phylogeny of eukaryotic phenylammonia lyases (PAL) and HALs with 100 bootstrap replicates; LG+G4 was chosen as model for protein evolution according to Bayesian Information Criterion. Sequences for PAL in plants have been identified using an HMM approach. Sequences from fungal PALs and eukaryote HALs have been selected from de Vries et al. (2017). Sequences from *A. thaliana* have been highlighted in pink, *A. filiculoides* is highlighted in blue, sequences from *S. bicolor* are indicated in black and TAM1 from *Oryza sativa* is highlighted in orange. Bootstrap support of 100 is indicated by black and colored dots on the branches. The clades with fungal PAL and plant tRNA synthase sequences have been collapsed. The substrate-specificity defining residues 123 and 443 of *S. bicolor* PTAL (Sb04g026510) have been analyzed for all sequences in the alignment and are indicated on the right next to the respective sequences. One exception is the collapsed branch of fungal PALs. Due to the variance of residue 123 the sequence logo for the two residues is printed on the branch itself.

Figure 3. Phylogeny of Hydratases in Chloroplastida. ML-phylogeny pointing the evolutionary history of AIM1/CHD hydratases in chloroplastida using 100 bootstrap replicates; LG+I+G4 was chosen as model for protein evolution according to Bayesian

Information Criterion. The AIM1 sequence of *A. thaliana* is highlighted in purple, its ortholog *Ph*CHD from *Petunia hybrida* is highlighted in light pink and sequence from *A. filiculoides* is highlighted in blue. Bootstrap levels = 100 are indicated by black dots.

Figure 4. ML-phylogeny determining the evolutionary history of KAT sequences in chloroplastida. The phylogeny is based on 100 bootstrap replicates; LG+I+G4 was chosen as model for protein evolution according to Bayesian Information Criterion. Sequences from *A. thaliana* are shown in purple, the *Ph*KAT sequence from *P. hybrida* is shown in light pink and the sequence from *A. filiculoides* is highlighted in blue. Clades with brassicaceae and angiosperm KAT sequences have been highlighted in purple, Solanaceae KAT sequences are indicated by a pink box and fern KAT sequences are indicated by a blue box. Bootstrap levels of a 100 are indicated by dots along the branches.

Figure 5. Phylogeny of the DHNAT family. ML-phylogeny was computed with IQ-Tree version multicore version 1.5.5 for Linux 64-bit with 100 bootstrap-replicates; JTT+I+G4 was chosen as model for protein evolution according to Bayesian Information Criterion. Bootstrap support of 100 is indicated by black and colored dots on the individual branches. DHNAT1 and 2 from *A. thaliana* are indicated in purple, the monophyletic DHNAT1 clade is highlighted in purple and the monophyletic DHNAT2 clade is highlighted in pink. DHNAT orthologs in ferns are highlighted in blue and the sequences from *A. filiculoides* is written in blue and bold.

Figure 6. Evolution of the AAO family. ML-phylogeny with 100 bootstrap replicates to recover the evolution of the AAO family; LG+F+I+G4 was chosen as model for protein evolution according to Bayesian Information Criterion. The blastp searches identified sequences either belonging to xanthin dehydrogenase (XDH) and AAO clades. The AAO clade is highlighted in purple and the XDH clade is highlighted in brown. Sequences from *A. thaliana* are indicated in pink and sequences from *A. filiculoides* are indicated in blue. Bootstrap support of 100 is indicated by black dots.

Figure 7. Routes of SA biosynthesis in land plants. SA can be derived from isochorismate or benzoic acid. The route from isochorismate requires ICS and a GH3 enzyme (Wildermuth et al., 2001, Garcion et al. 2008, Rekhter et al. 2019, Torrens-Spence et al. 2019), whereas the benzoic acid-derived SA pathway is less direct requires several steps that function also in other pathways. The reactions are indicated by arrows and the responsible enzymes are written on top of these arrows. Grey enzyme names indicate steps that have not been analyzed in this study because (i) data was available from previous

studies or (ii) sequences for these enzymes are not available from functionally characterized enzymes because there is only indirect evidence. Boxes below the arrows indicate the number of high-confidence sequences available in the genome of *A. filiculoides.* Grey boxes indicate absence in *A. filiculoides,* blue boxes indicate the presence of homologs in the fern and pink boxes indicate presence of orthologs encoded in the genome of *A. filiculoides.*

Figure 8. Chorismate-binding enzymes in cyanobacteria. (a) Three chorismate-binding enzymes, an isochorismate (ICS), anthranilate synthase (AS) and aminodeoxychorismate synthase (ADCS), were identified in *T. azollae* using a blastp search. Protein domains identified via TIGR are drawn to scale (blue= isochorismate synthase domain, yellow = anthranilate synthase component I, red = ADCS component I domain). Amino acid positions are indicated by the bar above. (b) Number of blastp hits for IPL in cyanobacteria, using the IPL sequence of *P. aeruginosa* sorted according to taxonomy. Hits recovering sequences from the Nostocales are highlighted by a brown box. (c) Number of hits recovered through a blastp search for salicylate synthase with the sequence from *M. tuberculosis* as query sorted according to cyanobacterial taxonomy. Hits to Nostocales are highlighted by a brown box. (d) Sequence logos for the conserved regions in chorismate binding enzymes. Highlighted in blue and orange are residues relevant for substrate specificity (Plach et al. 2015).

Figure 9. Differential gene expression of homologs of genes for SA biosynthesis and SA responses. (a) Differential gene expression of genes associated with the PAL-dependent pathway for SA biosynthesis in *A. filiculoides,* including candidates for *AfPAL, Af4CL, AfAAE clade VI* (i.e. the closest homologs to *AtBOZ1* and *PhCNL* in *A. filiculoides*), *AfAIM1, AfKAT, AfDHNAT, AfBALDH,* and *AfAAO4.* (b) Differential gene expression of homologs of SA-responsive genes. Significant differential regulation is indicated by blue and yellow colors. Light yellow indicates significant differential up-regulation (FDR ≤ 0.05) with a $\log_2$(FC) above 0 and below 1, dark yellow indicates significant differential up-regulation (FDR ≤ 0.05) with a $\log_2$(FC) above 1. Light blue indicates differential significant down-regulation (FDR ≤ 0.05) with a $\log_2$(FC) below 0 but above -1 and dark blue indicates significant down-regulation (FDR ≤ 0.05) with a $\log_2$(FC) below -1.

REFERENCES

Adebesin F., Widhalm J.R., Lynch J.H., McCoy R.M. & Dudareva N. (2018) A peroxisomal thioesterase plays auxiliary roles in plant β-oxidative benzoic acid metabolism. *The Plant Journal* **93**, 905–916.

Amborella Genome Project (2013) The *Amborella* genome and the evolution of flowering plants. *Science,* 342, 1241089

917 Ankenbauer R.G. & Cox C.D. (1988) Isolation and characterization of Pseudomonas
918 aeruginosa mutants requiring salicylic acid for pyochelin biosynthesis. *Journal of*
919 *Bacteriology* **170**, 5364–5367.
920 Argout, X., Salse, J., Aury, J.-M., Guiltinan, M. J., Droc, G., Gouzy, J., … Lanaud, C. (2011).
921 The genome of *Theobroma cacao*. *Nature Genetics*, 43, 101–108.
922 Arnerup J., Nemesio-Gorriz M., Lundén K., Asiegbu F.O., Stenlid J. & Elfstrand M. (2012)
923 The primary module in Norway spruce defence signalling against H. annosum s.l.
924 seems to be jasmonate-mediated signalling without antagonism of salicylate-mediated
925 signalling. *Planta* **237**, 1037–1045.
926 Banks, J. A., Nishiyama, T., Hasebe, M., Bowman, J.L., Gribskov, N., dePamhilis, C., Albert,
927 V. A., … Grigoriev, I. V. (2011). The Selaginella genome identifies genetic changes
928 associated with the evolution of vascular plants. *Science,* 332, 960-963.
929 Becking J.H. (1987) Endophyte transmission and activity in the Anabaena-Azolla
930 association. *Plant and Soil* **100**, 183–212.
931 Belton S., McCabe P.F. & Ng C.K.Y. (2021) The cyanobacterium, *Nostoc punctiforme* can
932 protect against programmed cell death and induce defence genes in *Arabidopsis*
933 *thaliana*. *Journal of Plant Interactions* **16**, 64–74.
934 Blilou I., Ocampo J., & García Garrido J. (1999) Resistance of pea roots to endomycorrhizal
935 fungus or *Rhizobium* correlates with enhanced levels of endogenous salicylic acid.
936 *Journal of Experimental Botany* **50**, 1663-1668.
937 Blilou I., Ocampo J., & Garcia-Garrido J. 2000. Induction of *Ltp* (lipid transfer protein) and
938 *PAL* (phenylalanine ammonia lyase) gene expression in rice roots colonized by the
939 arbuscular mycorrhizal fungus *Glomus mossae*. *Journal of Experimental Botany* **51**,
940 1969-1977.
941 Blum M., Chang H.-Y., Chuguransky S., Grego T., Kandasaamy S., Mitchell A., … Finn R.D.
942 (2021) The InterPro protein families and domains database: 20 years on. *Nucleic*
943 *Acids Research* **49**, D344–D354.
944 Block A., Widhalm J.R., Fatihi A., Cahoon R.E., Wamboldt Y., Elowsky C., … Basset G.J.
945 (2014) The Origin and Biosynthesis of the Benzenoid Moiety of Ubiquinone
946 (Coenzyme Q) in *Arabidopsis*. *The Plant Cell* **26**, 1938–1948.
947 Bowman, J. L., Kohchi, T., Yamato, K.T., Jenkins, J., Shu, S., Ishizaki, K., … Schmutz, J.
948 (2017). Insights into land plant evolution garnered from the *Marchantia polymorpha*
949 genome. *Cell*, 171, 287-304.
950 Brouwer P., Br utigam A., Buijs V.A., Tazelaar A.O.E., van der Werf A., Schlüter U., …
951 Schluepmann H. (2017) Metabolic Adaptation, a Specialized Leaf Organ Structure and
952 Vascular Responses to Diurnal N2 Fixation by Nostoc azollae Sustain the Astonishing

953 Productivity of Azolla Ferns without Nitrogen Fertilizer. *Frontiers in Plant Science* **8**, 15–
954 16.
955 Bussell J.D., Reichelt M., Wiszniewski A.A.G., Gershenzon J. & Smith S.M. (2014)
956 Peroxisomal ATP-Binding Cassette Transporter COMATOSE and the Multifunctional
957 Protein ABNORMAL INFLORESCENCE MERISTEM Are Required for the Production
958 of Benzoylated Metabolites in Arabidopsis Seeds. *Plant Physiology* **164**, 48–54.
959 Calvert H.E. & Peters G.A. (1981) The Azolla-Anabaena azollae relationship. *New*
960 *Phytologist* **89**, 327–335.
961 Calvert H.E., Pence M.K. & Peters G.A. (1985) Ultrastructural ontogeny of leaf cavity
962 trichomes in Azolla implies a functional role in metabolite exchange. *Protoplasma* **129**,
963 10–27.
964 Carpenter E.J., Matasci N., Ayyampalayam S., Wu S., Sun J., Yu J., … Wong G.K.-S.
965 (2019) Access to RNA-sequencing data from 1,173 plant species: The 1000 Plant
966 transcriptomes initiative (1KP). *GigaScience* **8**, giz126.
967 Carrapiço F (2006) Is the *Azolla-Anabaena* symbiosis a co-evolution case? In: Sitnykov A
968 (ed) *General botany: traditions and perspectives*. Kazan University, Kazan, pp 193–
969 195
970 Cheng, S., Xian, W., Fu, Y., Marin, B., Keller, J., Wu, T., … Melkonian, M. (2019) Genomes
971 of subaerial Zygnematophyceae provide insights into land plant evolution. *Cell,* 179,
972 1057-1067.e14.
973 Cochrane F.C., Davin L.B. & Lewis N.G. (2004) The Arabidopsis phenylalanine ammonia
974 lyase gene family: kinetic characterization of the four PAL isoforms. *Phytochemistry*
975 **65**, 1557–1564.
976 Collinson M.E. (2002) The ecology of Cainozoic ferns. *Review of Palaeobotany and*
977 *Palynology* **119**, 51–68.
978 Colquhoun T.A., Marciniak D.M., Wedde A.E., Kim J.Y., Schwieterman M.L., Levin L.A., …
979 Clark D.G. (2012) A peroxisomally localized acyl-activating enzyme is required for
980 volatile benzenoid formation in a Petunia×hybrida cv. 'Mitchell Diploid' flower. *Journal*
981 *of Experimental Botany* **63**, 4821–4833.
982 Coquoz J.-L., Buchala A. & Métraux J.-P. (1998) The Biosynthesis of Salicylic Acid in Potato
983 Plants. *Plant Physiology* **117**, 1095–1101.
984 Danielsson M., Lundén K., Elfstrand M., Hu J., Zhao T., Arnerup J., … Stenlid J. (2011)
985 Chemical and transcriptional responses of Norway spruce genotypes with different
986 susceptibility to Heterobasidion spp. infection. *BMC Plant Biology* **11**, 154.
987 Daruwala R., Kwon O., Meganathan R. & Hudspeth M.E.S. (1996) A new isochorismate
988 synthase specifically involved in menaquinone (vitamin K_2) biosynthesis encoded by
989 the *menF* gene. *FEMS Microbiology Letters* **140**, 159–163.

de Vries J., de Vries S., Slamovits C.H., Rose L.E. & Archibald J.M. (2017) How Embryophytic is the Biosynthesis of Phenylpropanoids and their Derivatives in Streptophyte Algae? *Plant and Cell Physiology* **58**, 934–945.

de Vries S., de Vries J., von Dahlen J.K., Gould S.B., Archibald J.M., Rose L.E. & Slamovits C.H. (2018) On plant defense signaling networks and early land plant evolution. *Communicative & Integrative Biology* **11**, 1–14.

de Vries S., de Vries J., Teschke H., von Dahlen J.K., Rose L.E. & Gould S.B. (2018) Jasmonic and salicylic acid response in the fern Azolla filiculoidesand its cyanobiont. *Plant, Cell & Environment* **41**, 2530–2548.

de Vries S. & de Vries J. (2018) Azolla: A Model System for Symbiotic Nitrogen Fixation and Evolutionary Developmental Biology. In *Current Advances in Fern Research*. pp. 21–46. Springer International Publishing, Cham.

de Vries J., Curtis B.A., Gould S.B. & Archibald J.M. (2018) Embryophyte stress signaling evolved in the algal progenitors of land plants. *Proceedings of the National Academy of Sciences of the United States of America* **115**, E3471–E3480.

de Vries J., Vries S., Curtis B.A., Zhou H., Penny S., Feussner K., … Archibald J.M. (2020) Heat stress response in the closest algal relatives of land plants reveals conserved stress signaling circuits. *The Plant Journal* **324**, 1064–24.

Deluc L., Barrieu F., Marchive C., Lauvergeat V., Decendit A., Richard T., … Hamdi S. (2006) Characterization of a grapevine R2R3-MYB transcription factor that regulates the phenylpropanoid pathway. *Plant Physiology* **140**, 499–511.

Ding Y., Sun T., Ao K., Peng Y., Zhang Y., Li X. & Zhang Y. (2018) Opposite roles of salicylic acid receptors NPR1 and NPR3/NPR4 in transcriptional regulation of plant immunity. *Cell* **173**, 1454-1467.e15.

Ding P. & Ding Y. (2020) Stories of Salicylic Acid: A Plant Defense Hormone. *Trends in Plant Science* **25**, 549–565.

Dijkhuizen L.W., Brouwer P., Bolhuis H., Reichart G.-J., Koppers N., Huettel B., … Schluepmann H. (2017) Is there foul play in the leaf pocket? The metagenome of floating fern Azollareveals endophytes that do not fix N 2but may denitrify. *New Phytologist* **217**, 453–466.

Eily A.N., Pryer K.M. & Li F.-W. (2019) A first glimpse at genes important to the Azolla–Nostoc symbiosis. *Symbiosis* **78**, 149–162.

El-Gebali S., Mistry J., Bateman A., Eddy S.R., Luciani A., Potter S.C., Qureshi M., Richardson L.J., Salazar G.A., Smart A., Sonnhammer E.L.L., Hirsh L., Paladin L., Piovesan D., Tosatto S.C.E., & Finn R.D. (2019) The Pfam protein families database in 2019. *Nucleic Acids Research* **47**, D427–D432.

1026 Fernández I., Merlos M., López-Ráez J.A., Martínez-Medina A., Ferrol N., Azcón C., … Pozo
1027 M.J. (2014) Defense Related Phytohormones Regulation in Arbuscular Mycorrhizal
1028 Symbioses Depends on the Partner Genotypes. *Journal of Chemical Ecology* **40**, 791–
1029 803.
1030 Fürst-Jansen J.M.R., de Vries S. & de Vries J. (2020) Evo-physio: on stress responses and
1031 the earliest land plants. *Journal of Experimental Botany* **66**, 4–16.
1032 Gaille C., Kast P., & Haas D. (2002) Salicylate biosynthesis in *Pseudomonas aeroginosa*.
1033 *The Journal of Biological Chemistry* **277**, 21768-21775.
1034 Garcion C., Lohmann A., Lamodière E., Catinot J., Buchala A., Doermann P. & Métraux J.-
1035 P. (2008) Characterization and Biological Function of the *ISOCHORISMATE*
1036 *SYNTHASE2* Gene of Arabidopsis. *Plant Physiology* **147**, 1279–1287.
1037 Gross J., Cho W.K., Lezhneva L., Falk J., Krupinska K., Shinozaki K., … Meurer J. (2006) A
1038 plant locus essential for phylloquinone (vitamin K1) biosynthesis originated from a
1039 fusion of four eubacterial genes. *Journal of Biological Chemistry* **281**, 17189–17196.
1040 Güngör E., Brouwer P., Dijkhuizen L.W., Shaffar D.C., Nierop K.G.J., Vos R.C.H., …
1041 Schluepmann H. (2021) *Azolla* ferns testify: seed plants and ferns share a common
1042 ancestor for leucoanthocyanidin reductase enzymes. *New Phytologist* **229**, 1118–
1043 1132.
1044 Hall J.W., Swanson N.P. (1968) Studies on fossil *Azolla*: *Azolla montana*, a Cretaceous
1045 megaspore with many small floats. *American Journal of Botany* **55**, 1055-1061.
1046 Hill D.J. (1989) The control of the cell cycle in microbial symbionts. *New Phytologist* **112**,
1047 175–184.
1048 Hori, K., Maruyama, F., Fujisawa, T., Togashi, T., Yamamoto, N., Seo, M., … Ohta, H.
1049 (2014). *Klebsormidium flaccidum* genome reveals primary factors for plant terrestrial
1050 adaptation. *Nature Communications*, 5, 3978.
1051 Ibdah M., Chen Y.-T., Wilkerson C.G. & Pichersky E. (2009) An Aldehyde Oxidase in
1052 Developing Seeds of Arabidopsis Converts Benzaldehyde to Benzoic Acid. *Plant*
1053 *Physiology* **150**, 416–423.
1054 Iven T., König S., Singh S., Braus-Stromeyer S.A., Bischoff M., Tietze L.F., Braus G.H.,
1055 Lipka V., Feussner I., Dröge-Laser W. (2012) Transcriptional activation and production
1056 of tryptophan-derived secondary metabolites in Arabidopsis roots contributes to the
1057 defense against the fungal vascular pathogen *Verticillium longisporum*. *Molecular*
1058 *Plant* **5**, 1389-1402.
1059 Jiao, C., Sørensen, I., Sun, X., Sun, H., Behar, H., Alseekh, S., … Rose, J. K. C. (2020). The
1060 *Penium margaritaceum* genome: hallmarks of the origins of land plants. *Cell*, 181,
1061 P1097-1111.E12

1062 Jones D.T., Taylor W.R. & Thornton J.M. (1992) The rapid generation of mutation data
1063 matrices from protein sequences. *Bioinformatics* **8**, 275–282.
1064 Jun S.-Y., Sattler S.A., Cortez G.S., Vermerris W., Sattler S.E. & Kang C. (2018)
1065 Biochemical and Structural Analysis of Substrate Specificity of a Phenylalanine
1066 Ammonia-Lyase. *Plant Physiology* **176**, 1452–1468.
1067 Kalyaanamoorthy S., Minh B.Q., Wong T.K.F., von Haeseler A. & Jermiin L.S. (2017)
1068 ModelFinder: fast model selection for accurate phylogenetic estimates. *Nature*
1069 *methods* **14**, 587–589.
1070 Katoh K. & Standley D.M. (2013) MAFFT Multiple Sequence Alignment Software Version 7:
1071 Improvements in Performance and Usability. *Molecular Biology and Evolution* **30**, 772–
1072 780.
1073 Klempien A., Kaminaga Y., Qualley A., Nagegowda D.A., Widhalm J.R., Orlova I., …
1074 Dudareva N. (2012) Contribution of CoA Ligases to Benzenoid Biosynthesis in Petunia
1075 Flowers. *The Plant Cell* **24**, 2015–2030.
1076 Kolappan S., Zwahlen J., Zhou R., Truglio J.J., Tonge P.J. & Kisker C. (2007) Lysine 190 Is
1077 the Catalytic Base in MenF, the Menaquinone-Specific Isochorismate Synthase from
1078 *Escherichia coli*□: Implications for an Enzyme Family †. *Biochemistry* **46**, 946–953.
1079 Kwon O. & Meganathan R. (2009) Biosynthesis of Menaquinone (Vitamin K_2) and
1080 Ubiquinone (Coenzyme Q). *EcoSal Plus* **3**.
1081 Lamesch, P., Berardini, T. Z., Li, D., Swarbreck, D., Wilks, C., Sasidharan, R., … Huala, E.
1082 (2011). The Arabidopsis Information Resource (TAIR): improved gene annotation and
1083 new tools. *Nucleic Acids Research*, 40, D1202-D1210.
1084 Lang, D., Ullrich, K. K., Murat, F., Fuchs, J., Jenkins, J., Haas, F. B., … Rensing, S. A.
1085 (2018) The *Physcomitrella patens* chromosome-scale assembly reveals moss genome
1086 structure and evolution. *The Plant Journal*, 93, 515–533.
1087 Le S.Q. & Gascuel O. (2008) An improved general amino acid replacement matrix.
1088 *Molecular Biology and Evolution* **25**, 1307–1320.
1089 Lee S., Kaminaga Y., Cooper B., Pichersky E., Dudareva N. & Chapple C. (2012)
1090 Benzoylation and sinapoylation of glucosinolate R-groups in Arabidopsis: *Acylation of*
1091 *glucosinolates in Arabidopsis*. *The Plant Journal* **72**, 411–422.
1092 Leon J., Shulaev V., Yalpani N., Lawton M.A. & Raskin I. (1995) Benzoic acid 2-hydroxylase,
1093 a soluble oxygenase from tobacco, catalyzes salicylic acid biosynthesis. *Proceedings*
1094 *of the National Academy of Sciences* **92**, 10413–10417.
1095 Li F.-W., Brouwer P., Carretero-Paulet L., Cheng S., de Vries J., Delaux P.-M., … Pryer K.M.
1096 (2018) Fern genomes elucidate land plant evolution and cyanobacterial symbioses.
1097 *Nature Plants* **4**, 460–472.

1098 Li F.-W., Nishiyama T., Waller M., Frangedakis E., Keller J., Li Z., … Szövényi P. (2020)
1099 Anthoceros genomes illuminate the origin of land plants and the unique biology of
1100 hornworts. *Nature Plants* **6**, 259–272.
1101 Liu J., Blaylock L., Endre G., Cho J., Town C., VandenBosch K., & Harrison M. (2003)
1102 Transcript profiling coupled with spatial expression analysis reveals genes involved in
1103 distinct developmental stages of the arbuscular mycorrhizal symbiosis. *The Plant Cell*
1104 **15**, 2106-2123.
1105 Long M.C., Nagegowda D.A., Kaminaga Y., Ho K.K., Kish C.M., Schnepp J., … Dudareva N.
1106 (2009) Involvement of snapdragon benzaldehyde dehydrogenase in benzoic acid
1107 biosynthesis. *The Plant Journal* **59**, 256–265.
1108 Matyash V, Liebisch G, Kurzchalia TV, Shevchenko A, Schwudke D (2008) Lipid extraction
1109 by methyl-tert-butyl ether for high-throughput lipidomics. *Journal of Lipid Research* **49**,
1110 1137-1146.
1111 Marchler-Bauer A. & Bryant S.H. (2004) CD-Search: protein domain annotations on the fly.
1112 *Nucleic Acids Research* **32**, W327–W331.
1113 Meeks J.C., Elhai J., Thiel T., Potts M., Larimer F., Lamerdin J., Predki P., & Atlas R. (2001)
1114 An overview of the genome of *Nostoc punctiforme*, a multicellular, symbiotic
1115 cyanobacterium. *Photosynthesis Research* **70**, 85–106.
1116 Meuwly P., Molders W., Buchala A. & MCtraux J.-P. (1995) Local and systemic biosynthesis
1117 of salicylic acid in infected cucumber plants. *Plant Physiology* **109**, 1107-1114.
1118 Mistry J., Finn R.D., Eddy S.R., Bateman A. & Punta M. (2013) Challenges in homology
1119 search: HMMER3 and convergent evolution of coiled-coil regions. *Nucleic Acids*
1120 *Research* **41**, e121–e121.
1121 Nguyen L.-T., Schmidt H.A., von Haeseler A. & Minh B.Q. (2015) IQ-TREE: A Fast and
1122 Effective Stochastic Algorithm for Estimating Maximum-Likelihood Phylogenies.
1123 *Molecular Biology and Evolution* **32**, 268–274.
1124 Ni J., Dong L., Jiang Z., Yang X., Sun Z., Li J., … Xu M. (2018) Salicylic acid-induced
1125 flavonoid accumulation in *Ginkgo biloba* leaves is dependent on red and far-red light.
1126 *Industrial Crops and Products* **118**, 102–110.
1127 Nishiyama, T., Sakayama, H., de Vries, J., Buschmann, H., Saint-Marcoux, D., Ullrich, K. K.,
1128 … Rensing, S. A. (2018). The *Chara* genome: secondary complexity and implications
1129 for plant terrestrialization. *Cell*, 174, 448–464.
1130 Nugroho L.H., Verberne M.C. & Verpoorte R. (2002) Activities of enzymes involved in the
1131 phenylpropanoid pathway in constitutively salicylic acid-producing tobacco plants. *Plant*
1132 *Physiology and Biochemistry* **40**, 755–760.

1133 Nystedt, B., Street, N. R., Wetterbom, A., Zuccolo, A., Lin, Y.-C., Scofield, D. G., …
1134 Jansson, S. (2013). The Norway spruce genome sequence and conifer genome
1135 evolution. *Nature*, 497, 579-584.
1136 Ouyang, S., Zhu, W., Hamilton, J., Lin, H., Campbell, M., Childs, K., … Buell, C. R. (2007).
1137 The TIGR Rice Genome Annotation Resource: improvements and new features. *Nucleic*
1138 *Acids Research*, 35, D883–D887.
1139 Pallas J.A., Paiva N.L., Lamb C. & Dixon R.A. (1996) Tobacco plants epigenetically
1140 suppressed in phenylalanine ammonia-lyase expression do not develop systemic
1141 acquired resistance in response to infection by tobacco mosaic virus. *The Plant*
1142 *Journal* **10**, 281–293.
1143 Pereira A.L. & Vasconcelos V. (2014). Classification and phylogeny of the cyanobiont
1144 *Anabaena azollae* Strasburger: An answered question? *International Journal of*
1145 *Systematic and Evolutionary Microbiology*, 64, 1830–1840.
1146 Peters G.A., Toia R.E., Raveed D. & Levine N.J. (1978) The *Azolla-Anabaena azollae*
1147 relationship. VI. Morphological aspects of the association. *New Phytologist* **80**, 583–
1148 593.
1149 Peters G.A. & Meeks J.C. (1989) The Azolla-Anabaena symbiosis: basic biology. *Annual*
1150 *Review of Plant Biology* **40**, 193–210.
1151 Pereira, A. L., & Carrapiço, F. (2007). Histochemistry of simple hairs from the foliar cavities
1152 of Azolla filiculoides. *Plant Biosystems*, **141**, 323–328.
1153 Perkins S.K. & Peters G.A. (1993) The Azolla–Anabaena symbiosis: endophyte continuity in
1154 the Azolla life-cycle is facilitated by epidermal trichomes. *New Phytologist* **123**, 53–64.
1155 Plach M.G., Löffler P., Merkl R. & Sterner R. (2015) Conversion of Anthranilate Synthase
1156 into Isochorismate Synthase: Implications for the Evolution of Chorismate-Utilizing
1157 Enzymes. *Angewandte Chemie International Edition* **54**, 11270–11274.
1158 Plett J.M. & Martin F.M. (2018) Know your enemy, embrace your friend: using omics to
1159 understand how plants respond differently to pathogenic and mutualistic
1160 microorganisms. *The Plant Journal* **93**, 729–746.
1161 Ponce De León I., Schmelz E.A., Gaggero C., Castro A., Álvarez A. & Montesano M. (2012)
1162 Physcomitrella patens activates reinforcement of the cell wall, programmed cell death
1163 and accumulation of evolutionary conserved defence signals, such as salicylic acid
1164 and 12-oxo-phytodienoic acid, but not jasmonic acid, upon Botrytis cinerea infection:
1165 P. patens defence responses against B. cinerea. *Molecular Plant Pathology* **13**, 960–
1166 974.
1167 Pozo M.J., López-Ráez J.A., Azcón-Aguilar C., & García-Garrido J.M. (2015) Phytohormone
1168 as integrators of environmental signals in the regulation of mycorrhizal symbiosis. *New*
1169 *Phytologist* **205**, 1431-1436.

Qualley A.V., Widhalm J.R., Adebesin F., Kish C.M. & Dudareva N. (2012) Completion of the core -oxidative pathway of benzoic acid biosynthesis in plants. *Proceedings of the National Academy of Sciences* **109**, 16383–16388.

Rai A.N., Soderback E. & Bergman B. (2000) Cyanobacterium-plant symbioses. *New Phytologist* **147**, 449–481.

Ran L., Larsson J., Vigil-Stenman T., Nylander J.A.A., Ininbergs K., Zheng W.-W., … Bergman B. (2010) Genome Erosion in a Nitrogen-Fixing Vertically Transmitted Endosymbiotic Multicellular Cyanobacterium. *PLoS ONE* **5**, e11486.

Reboledo G., d Agorio A., Vignale L., Batista-García R.A., Ponce De León I. (2021) Transriptional profiling reveals conserved and species-specific plant defense responses during the interaction of *Physcomitrium patens* with *Botrytis cinerea*. *Plant Molecular Biology* https://doi.org/10.1007/s11103-021-01116-0

Rekhter D., Lüdke D., Ding Y., Feussner K., Zienkiewicz K., Lipka V., … Feussner I. (2019) Isochorismate-derived biosynthesis of the plant stress hormone salicylic acid. *Science* **365**, 498–502.

Rippka R., Deruelles J., Waterbury J.B., Herdman M. & Stanier R.Y. (1979) Generic assignments, strain histories and properties of pure cultures of cyanobacteria. *Journal of General Microbiology* 111, 1–61.

Robinson M.D. & Oshlack A. (2010) A scaling normalization method for differential expression analysis of RNA-seq data. *Genome Biology* **11**, R25.

Robinson M.D., McCarthy D.J., & Smyth G.K. (2010) edgeR: A bioconductor package for differential expression analysis of digital gene expression data. *Bioinformatics* 26: 139–140.

Shapiro S.S. & Wilk M.B. (1965) An analysis of variance test for normality (complete samples). *Biometrika*, 591–611.

Shen H., Jin D., Shu J.-P., Zhou X.-L., Lei M., Wei R., … Yan Y.-H. (2018) Large-scale phylogenomic analysis resolves a backbone phylogeny in ferns. *GigaScience* **7**.

Shi D.-J. & Hall D.O. (1988) TheAzolla-Anabaena association: Historical perspective, symbiosis and energy metabolism. *The Botanical Review* **54**, 353–386.

Shockey J.M., Fulda M.S. & Browse J. (2003) Arabidopsis contains a large superfamily of acyl-activating enzymes. Phylogenetic and biochemical analysis reveals a new class of acyl-coenzyme a synthetases. *Plant Physiology* **132**, 1065–1076.

Sierro, N. Battey, J., Ouadi, S., Bakaher, N., Bovet, L., Willig, A., Goepfert, S., Peitsch, M. C., & Ivanov, N. V. (2014). The tobacco genome sequence and its comparison with those of tomato and potato. *Nature Communications*, 5, 3833.

Slotte, T., Hazzouri, K. M., Ågren, J. A., Koenig, D., Maumus, F., Guo, Y.-L., … Wrigth, S. I. (2013). The *Capsella rubella* genome and the genomic consequences of rapid mating system evolution. *Nature Genetics*, 45, 831–835

Student (1908) The probable error of a mean. *Biometrika* **6**, 1–25.

The International *Brachypodium* Initiative. (2010). Genome sequencing and analysis of the model grass Brachypodium distachyon. *Nature*, 463, 763–768.

Toribio A.J., Suárez-Estrella F., Jurado M.M., López M.J., López-González J.A. & Moreno J. (2020) Prospection of cyanobacteria producing bioactive substances and their application as potential phytostimulating agents. *Biotechnology Reports* **26**, e00449.

Torrens-Spence M.P., Bobokalonova A., Carballo V., Glinkerman C.M., Pluskal T., Shen A. & Weng J.-K. (2019) PBS3 and EPS1 Complete Salicylic Acid Biosynthesis from Isochorismate in Arabidopsis. *Molecular Plant* **12**, 1577–1586.

Tounekti T., Hernández I. & Munné-Bosch S. (2013) Salicylic Acid Biosynthesis and Role in Modulating Terpenoid and Flavonoid Metabolism in Plant Responses to Abiotic Stress. In *Salicylic Acid*. (eds S. Hayat, A. Ahmad & M.N. Alyemeni), pp. 141–162. Springer Netherlands, Dordrecht.

Van Moerkercke A., Schauvinhold I., Pichersky E., Haring M.A. & Schuurink R.C. (2009) A plant thiolase involved in benzoic acid biosynthesis and volatile benzenoid production. *The Plant Journal* **60**, 292–302.

Visca P., Ciervo A., Sanfilippo V. & Orsi N. (1993) Iron-regulated salicylate synthesis by *Pseudomonas* spp. *Journal of General Microbiology* **139**, 1995–2001.

Vlot A.C., Dempsey D.M.A., & Klessig D.F. (2009). Salicylic acid, a multifaceted hormone to combat disease. *Annual Review of Phytopathology* **47**, 177-206.

Wan, T. et al. (2018). A genome for gnetophytes and early evolution of seed plants. *Nature Plants*, 4, 82–89.

Wang, S., Li, L., Li, H., Sahu, S. K., Wang, H., Xu, Y., … Liu, X. (2020) Genomes of early-diverging streptophyte algae shed light on plant terrestrialization. *Nature Plants*, **6**, 95-106.

Warshan D., Espinoza J.L., Stuart R.K., Richter R.A., Kim S.-Y., Shapiro N., … Rasmussen U. (2017) Feathermoss and epiphytic Nostoc cooperate differently: expanding the spectrum of plant–cyanobacteria symbiosis. *The ISME Journal* **11**, 2821–2833.

Weisshaar B. & Jenkins G.I. (1998) Phenylpropanoid biosynthesis and its regulation. *Current Opinion in Plant Biology* **1**, 251–257.

Wildermuth M.C., Dewdney J., Wu G. & Ausubel F.M. (2001) Isochorismate synthase is required to synthesize salicylic acid for plant defence. *Nature* **414**, 562–565.

Widhalm J.R., Ducluzeau A.-L., Buller N.E., Elowsky C.G., Olsen L.J. & Basset G.J.C. (2012) Phylloquinone (vitamin K1) biosynthesis in plants: two peroxisomal

1242 thioesterases of lactobacillales origin hydrolyze 1,4-dihydroxy-2-naphthoyl-coa: Plant
1243 DHNA-CoA thioesterases. *The Plant Journal* **71**, 205–215.
1244 Widhalm J.R. & Dudareva N. (2015) A Familiar Ring to It: Biosynthesis of Plant Benzoic
1245 Acids. *Molecular Plant* **8**, 83–97.
1246 Yan J., Aboshi T., Teraishi M., Strickler S.R., Spindel J.E., Tung C.-W., … Jander G. (2015)
1247 The Tyrosine Aminomutase TAM1 Is Required for β-Tyrosine Biosynthesis in Rice.
1248 *The Plant Cell* **27**, 1265–1278.
1249 Zheng W., Bergman B., Chen B., Zheng S., Xiang G. & Rasmussen U. (2009a) Cellular
1250 responses in the cyanobacterial symbiont during its vertical transfer between plant
1251 generations in the Azolla microphyllasymbiosis. *New Phytologist* **181**, 53–61.
1252 Zheng W., Rang L., Bergman B. (2009b) Structural Characteristics of the Cyanobacterium–
1253 Azolla Symbioses. In: Pawlowski K. (eds) Prokaryotic Symbionts in Plants.
1254 *Microbiology Monographs*, vol 8. Springer, Berlin, Heidelberg.
1255 Zwahlen J., Kolappan S., Zhou R., Kisker C. & Tonge P.J. (2007) Structure and Mechanism
1256 of MbtI, the Salicylate Synthase from *Mycobacterium tuberculosis* †. *Biochemistry* **46**,
1257 954–964.
1258

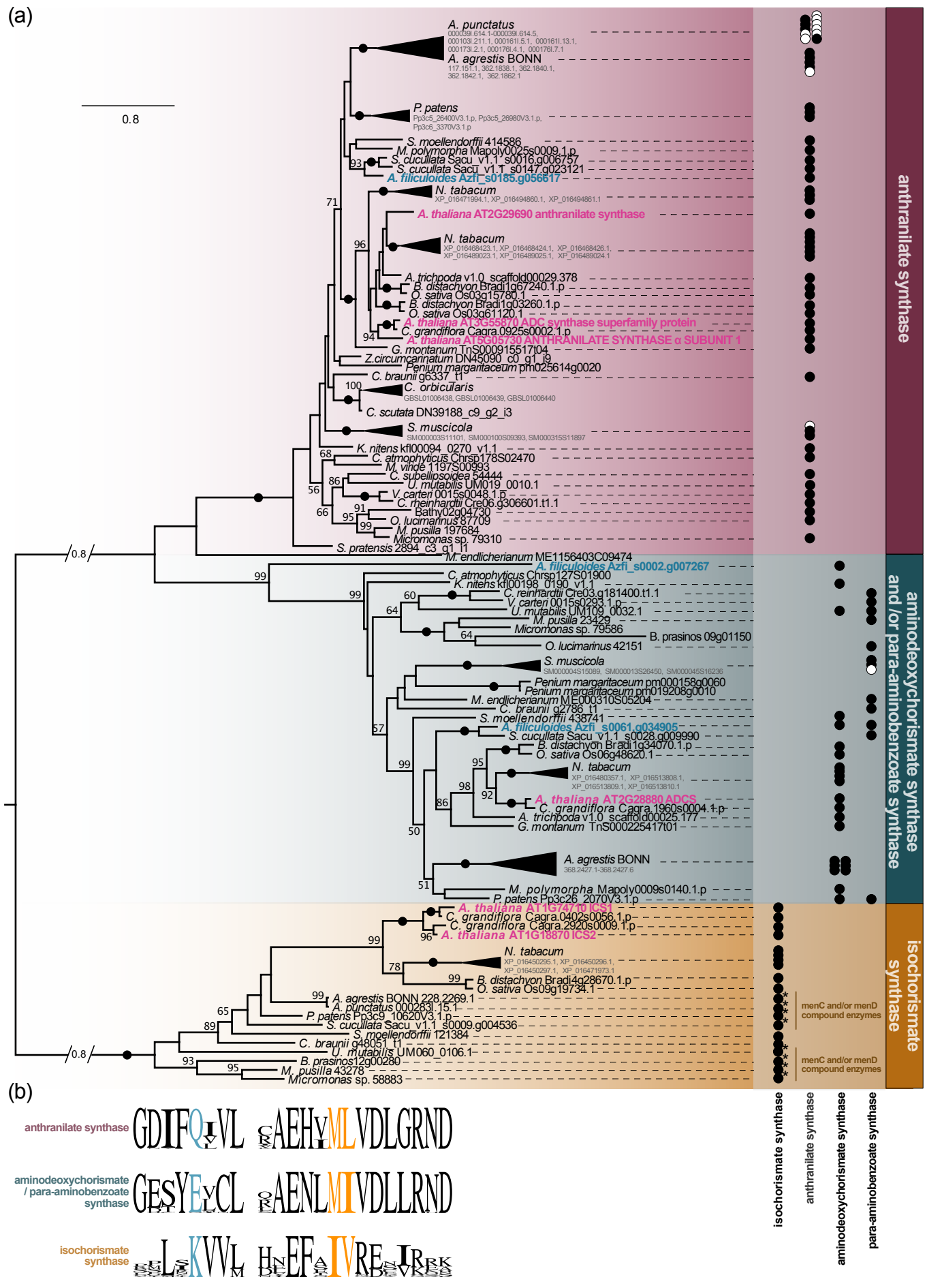
(a)
0.8
A. punctatus
000039I.614.1-000039I.614.5, 000103I.211.1, 000161I.5.1, 000161I.13.1, 000173I.2.1, 000176I.4.1, 000176I.7.1
A. agrestis BONN
117.151.1, 362.1838.1, 362.1840.1, 362.1842.1, 362.1862.1
P. patens
Pp3c5_26400V3.1.p, Pp3c5_26980V3.1.p, Pp3c6_3370V3.1.p
S. moellendorffii 414586
M. polymorpha Mapoly0025s0009.1.p
S. cucullata Sacu_v1.1_s0016.g006757
S. cucullata Sacu_v1.1_s0147.g023121
A. filiculoides Azfi_s0185.g056617
N. tabacum
XP_016471994.1, XP_016494860.1, XP_016494861.1
A. thaliana AT2G29690 anthranilate synthase
N. tabacum
XP_016468423.1, XP_016468424.1, XP_016468426.1, XP_016489023.1, XP_016489025.1, XP_016489024.1
A. trichopoda v1.0_scaffold00029.378
B. distachyon Bradi1g67240.1.p
O. sativa Os03g0157800.1
B. distachyon Bradi1g03260.1.p
O. sativa Os03g61120.1
A. thaliana AT3G55570 ADC synthase superfamily protein
C. grandiflora Cagra.0925s0002.1.p
A. thaliana AT5G05730 ANTHRANILATE SYNTHASE α SUBUNIT 1
G. montanum TnS000915517t04
Z.circumcarinatum DN45090_c0_g1_i9
Penium margaritaceum pm025614g0020
C. braunii g6337_t1
C. orbicularis
GBSL01006438, GBSL01006439, GBSL01006440
C. scutata DN39188_c9_g2_i3
S. muscicola
SM000003S11101, SM000100S09393, SM000315S11897
K. nitens kfl00094_0270_v1.1
C. atmophyticus Chrsp178S02470
M. viride 197S00993
C. subellipsoidea 54444
U. mutabilis UM019_0010.1
V. carteri 0015s0048.1.p
C. rheinhardtii Cre06.g306601.t1.1
Bathy02g04730
O. lucimarinus 87709
M. pusilla 197684
Micromonas sp. 79310
S. pratensis 2894_c3_g1_i1
M. endlicherianum ME1156403C09474
A. filiculoides Azfi_s0002.g007267
C. atmophyticus Chrsp127S01900
K. nitens kfl00198_0190_v1.1
C. reinhardtii Cre03.g181400.t1.1
V. carteri 0015s0293.1.p
U. mutabilis UM109_0032.1
M. pusilla 23429
Micromonas sp. 79586
B. prasinos 09g01150
O. lucimarinus 42151
S. muscicola
SM000004S15089, SM000013S26450, SM000045S16236
Penium margaritaceum pm000158g0060
Penium margaritaceum pm019208g0010
M. endlicherianum ME000310S05204
C. braunii g2786_t1
S. moellendorffii 438741
A. filiculoides Azfi_s0061.g034905
S. cucullata Sacu_v1.1_s0028.g009990
B. distachyon Bradi1g34070.1.p
O. sativa Os06g48620.1
N. tabacum
XP_016480357.1, XP_016513808.1, XP_016513809.1, XP_016513810.1
A. thaliana AT2G28880 ADCS
C. grandiflora Cagra.1960s0004.1.p
A. trichopoda v1.0_scaffold00025.177
G. montanum TnS000225417t01
A. agrestis BONN
368.2427.1-368.2427.6
M. polymorpha Mapoly0009s0140.1.p
P. patens Pp3c26_2070V3.1.p
A. thaliana AT1G74710 ICS1
C. grandiflora Cagra.0402s0056.1.p
C. grandiflora Cagra.2920s0009.1.p
A. thaliana AT1G18870 ICS2
N. tabacum
XP_016450295.1, XP_016450296.1, XP_016450297.1, XP_016471973.1
B. distachyon Bradi4g28670.1.p
O. sativa Os09g19734.1
A. agrestis BONN 228.2269.1
A. punctatus 000283I.15.1
P. patens Pp3c9_10620V3.1.p
S. cucullata Sacu_v1.1_s0009.g004536
S. moellendorffii 121384
C. braunii g48051_t1
U. mutabilis UM060_0106.1
B. prasinos12g00280
M. pusilla 43278
Micromonas sp. 58883
anthranilate synthase
aminodeoxychorismate synthase and/or para-aminobenzoate synthase
isochorismate synthase
menC and/or menD compound enzymes
menC and/or menD compound enzymes
(b)
anthranilate synthase
aminodeoxychorismate / para-aminobenzoate synthase
isochorismate synthase
isochorismate synthase
anthranilate synthase
aminodeoxychorismate synthase
para-aminobenzoate synthase

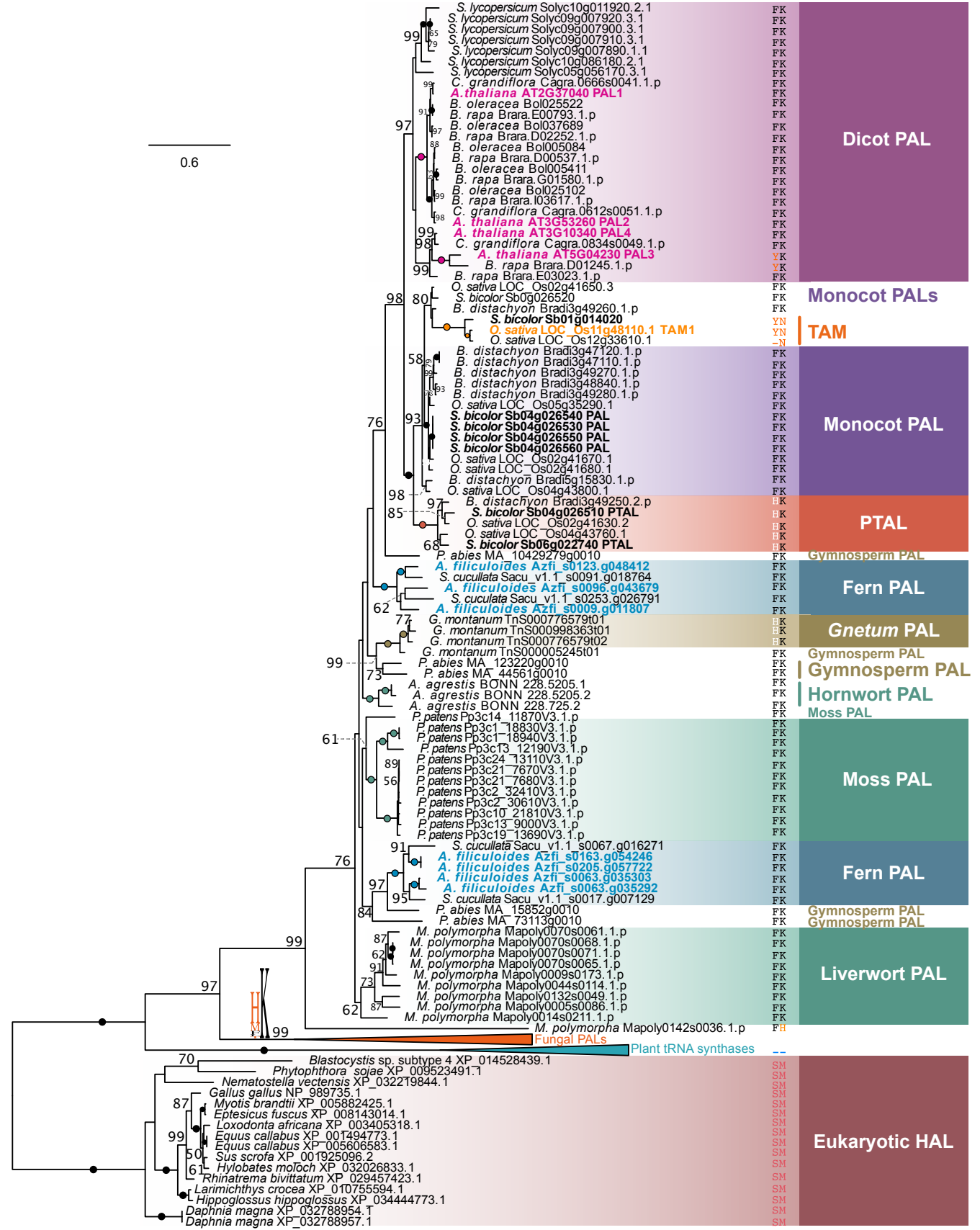
0.6
S. lycopersicum Solyc10g011920.2.1
S. lycopersicum Solyc09g007920.3.1
S. lycopersicum Solyc09g007900.3.1
S. lycopersicum Solyc09g007910.3.1
S. lycopersicum Solyc09g007890.1.1
S. lycopersicum Solyc10g086180.2.1
S. lycopersicum Solyc05g056170.3.1
C. grandiflora Cagra.0666s0041.1.p
A.thaliana AT2G37040 PAL1
B. oleracea Bol025522
B. rapa Brara.E00793.1.p
B. oleracea Bol037689
B. rapa Brara.D02252.1.p
B. oleracea Bol005084
B. rapa Brara.D00537.1.p
B. oleracea Bol005411
B. rapa Brara.G01580.1.p
B. oleracea Bol025102
B. rapa Brara.I03617.1.p
C. grandiflora Cagra.0612s0051.1.p
A. thaliana AT3G53260 PAL2
A. thaliana AT3G10340 PAL4
C. grandiflora Cagra.0834s0049.1.p
A. thaliana AT5G04230 PAL3
B. rapa Brara.D01245.1.p
B. rapa Brara.E03023.1.p
Dicot PAL
O. sativa LOC_Os02g41650.3
S. bicolor Sb0g026520
B. distachyon Bradi3g49260.1.p
Monocot PALs
S. bicolor Sb01g014020
O. sativa LOC_Os11g48110.1 TAM1
O. sativa LOC_Os12g33610.1
TAM
B. distachyon Bradi3g47120.1.p
B. distachyon Bradi3g47110.1.p
B. distachyon Bradi3g49270.1.p
B. distachyon Bradi3g48840.1.p
B. distachyon Bradi3g49280.1.p
O. sativa LOC_Os05g35290.1
S. bicolor Sb04g026540 PAL
S. bicolor Sb04g026530 PAL
S. bicolor Sb04g026550 PAL
S. bicolor Sb04g026560 PAL
O. sativa LOC_Os02g41670.1
O. sativa LOC_Os02g41680.1
B. distachyon Bradi5g15830.1.p
O. sativa LOC_Os04g43800.1
Monocot PAL
B. distachyon Bradi3g49250.2.p
S. bicolor Sb04g026510 PTAL
O. sativa LOC_Os02g41630.2
O. sativa LOC_Os04g43760.1
S. bicolor Sb06g022740 PTAL
PTAL
P. abies MA_10429279g0010
Gymnosperm PAL
A. filiculoides Azfi_s0123.g048412
S. cucullata Sacu_v1.1_s0091.g018764
A. filiculoides Azfi_s0096.g043679
S. cuculata Sacu_v1.1_s0253.g026791
A. filiculoides Azfi_s0009.g011807
Fern PAL
G. montanum TnS000776579t01
G. montanum TnS000998363t01
G. montanum TnS000776579t02
Gnetum PAL
G. montanum TnS000005245t01
P. abies MA_123220g0010
P. abies MA_44561g0010
Gymnosperm PAL
Gymnosperm PAL
A. agrestis BONN_228.5205.1
A. agrestis BONN_228.5205.2
A. agrestis BONN_228.725.2
Hornwort PAL
Moss PAL
P. patens Pp3c14_11870V3.1.p
P. patens Pp3c1_18830V3.1.p
P. patens Pp3c1_18940V3.1.p
P. patens Pp3c13_12190V3.1.p
P. patens Pp3c24_13110V3.1.p
P. patens Pp3c21_7670V3.1.p
P. patens Pp3c21_7680V3.1.p
P. patens Pp3c2_32410V3.1.p
P. patens Pp3c2_30610V3.1.p
P. patens Pp3c10_21810V3.1.p
P. patens Pp3c13_9000V3.1.p
P. patens Pp3c19_13690V3.1.p
Moss PAL
S. cucullata Sacu_v1.1_s0067.g016271
A. filiculoides Azfi_s0163.g054246
A. filiculoides Azfi_s0205.g057722
A. filiculoides Azfi_s0063.g035303
A. filiculoides Azfi_s0063.g035292
S. cucullata Sacu_v1.1_s0017.g007129
Fern PAL
P. abies MA_15852g0010
P. abies MA_73113g0010
Gymnosperm PAL
Gymnosperm PAL
M. polymorpha Mapoly0070s0061.1.p
M. polymorpha Mapoly0070s0068.1.p
M. polymorpha Mapoly0070s0071.1.p
M. polymorpha Mapoly0070s0065.1.p
M. polymorpha Mapoly0009s0173.1.p
M. polymorpha Mapoly0044s0114.1.p
M. polymorpha Mapoly0132s0049.1.p
M. polymorpha Mapoly0005s0086.1.p
M. polymorpha Mapoly0014s0211.1.p
Liverwort PAL
M. polymorpha Mapoly0142s0036.1.p
Fungal PALs
Plant tRNA synthases
Blastocystis sp. subtype 4 XP_014528439.1
Phytophthora_sojae XP_009523491.1
Nematostella vectensis XP_032219844.1
Gallus gallus NP_989735.1
Myotis brandtii XP_005882425.1
Eptesicus fuscus XP_008143014.1
Loxodonta africana XP_003405318.1
Equus callabus XP_001494773.1
Equus callabus XP_005606583.1
Sus scrofa XP_001925096.2
Hylobates moloch XP_032026833.1
Rhinatrema bivittatum XP_029457423.1
Larimichthys crocea XP_010755594.1
Hippoglossus hippoglossus XP_034444773.1
Daphnia magna XP_032788954.1
Daphnia magna XP_032788957.1
Eukaryotic HAL

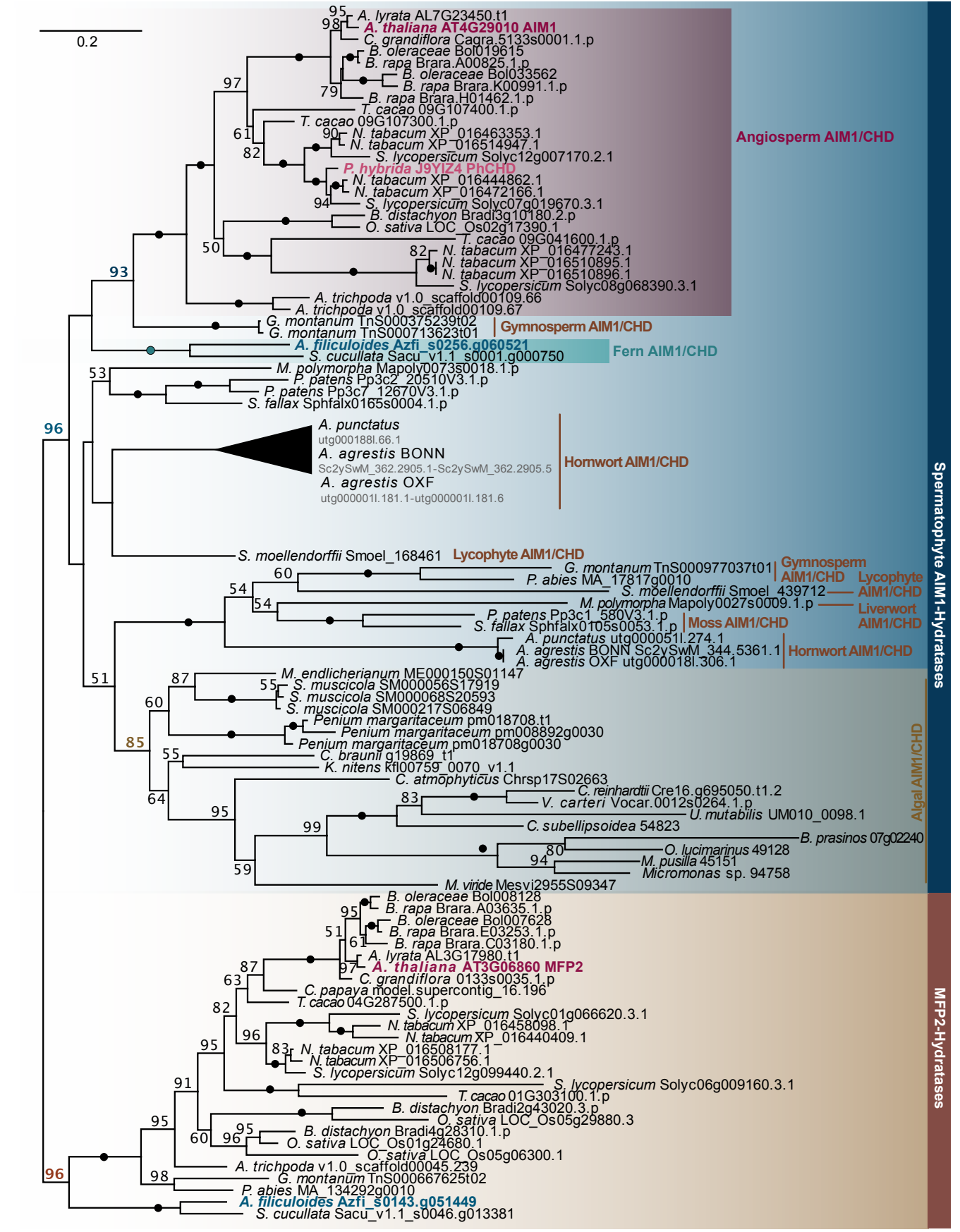
0.2
A. lyrata AL7G23450.t1
A. thaliana AT4G29010 AIM1
C. grandiflora Cagra.5133s0001.1.p
B. oleraceae Bol019615
B. rapa Brara.A00825.1.p
B. oleraceae Bol033562
B. rapa Brara.K00991.1.p
B. rapa Brara.H01462.1.p
T. cacao 09G107400.1.p
T. cacao 09G107300.1.p
N. tabacum XP_016463353.1
N. tabacum XP_016514947.1
S. lycopersicum Solyc12g007170.2.1
P. hybrida J9YIZ4 PhCHD
N. tabacum XP_016444862.1
N. tabacum XP_016472166.1
S. lycopersicum Solyc07g019670.3.1
B. distachyon Bradi3g10180.2.p
O. sativa LOC_Os02g17390.1
T. cacao 09G041600.1.p
N. tabacum XP_016477243.1
N. tabacum XP_016510895.1
N. tabacum XP_016510896.1
S. lycopersicum Solyc08g068390.3.1
A. trichpoda v1.0_scaffold00109.66
A. trichpoda v1.0_scaffold00109.67
G. montanum TnS000375239t02
G. montanum TnS000713623t01
A. filiculoides Azfi_s0256.g060521
S. cucullata Sacu_v1.1_s0001.g000750
M. polymorpha Mapoly0073s0018.1.p
P. patens Pp3c2_20510V3.1.p
P. patens Pp3c7_12670V3.1.p
S. fallax Sphfalx0165s0004.1.p
A. punctatus
utg000188l.66.1
A. agrestis BONN
Sc2ySwM_362.2905.1-Sc2ySwM_362.2905.5
A. agrestis OXF
utg000001l.181.1-utg000001l.181.6
S. moellendorffii Smoel_168461
G. montanum TnS000977037t01
P. abies MA_17817g0010
S. moellendorffii Smoel_439712
M. polymorpha Mapoly0027s0009.1.p
P. patens Pp3c1_580V3.1.p
S. fallax Sphfalx0105s0053.1.p
A. punctatus utg000051l.274.1
A. agrestis BONN Sc2ySwM_344.5361.1
A. agrestis OXF utg000018l.306.1
M. endlicherianum ME000150S01147
S. muscicola SM000056S17919
S. muscicola SM000068S20593
S. muscicola SM000217S06849
Penium margaritaceum pm018708.t1
Penium margaritaceum pm008892g0030
Penium margaritaceum pm018708g0030
C. braunii g19869_t1
K. nitens kfl00759_0070_v1.1
C. atmophyticus Chrsp17S02663
C. reinhardtii Cre16.g695050.t1.2
V. carteri Vocar.0012s0264.1.p
U. mutabilis UM010_0098.1
C. subellipsoidea 54823
B. prasinos 07g02240
O. lucimarinus 49128
M. pusilla 45151
Micromonas sp. 94758
M. viride Mesvi2955S09347
B. oleraceae Bol008128
B. rapa Brara.A03635.1.p
B. oleraceae Bol007628
B. rapa Brara.E03253.1.p
B. rapa Brara.C03180.1.p
A. lyrata AL3G17980.t1
A. thaliana AT3G06860 MFP2
C. grandiflora 0133s0035.1.p
C. papaya model.supercontig_16.196
T. cacao 04G287500.1.p
S. lycopersicum Solyc01g066620.3.1
N. tabacum XP_016458098.1
N. tabacum XP_016440409.1
N. tabacum XP_016508177.1
N. tabacum XP_016506756.1
S. lycopersicum Solyc12g099440.2.1
S. lycopersicum Solyc06g009160.3.1
T. cacao 01G303100.1.p
B. distachyon Bradi2g43020.3.p
O. sativa LOC_Os05g29880.3
B. distachyon Bradi4g28310.1.p
O. sativa LOC_Os01g24680.1
O. sativa LOC_Os05g06300.1
A. trichpoda v1.0_scaffold00045.239
G. montanum TnS000667625t02
P. abies MA_134292g0010
A. filiculoides Azfi_s0143.g051449
S. cucullata Sacu_v1.1_s0046.g013381
Angiosperm AIM1/CHD
Gymnosperm AIM1/CHD
Fern AIM1/CHD
Hornwort AIM1/CHD
Lycophyte AIM1/CHD
Gymnosperm AIM1/CHD
Lycophyte AIM1/CHD
Liverwort AIM1/CHD
Moss AIM1/CHD
Hornwort AIM1/CHD
Algal AIM1/CHD
Spermatophyte AIM1-Hydratases
MFP2-Hydratases

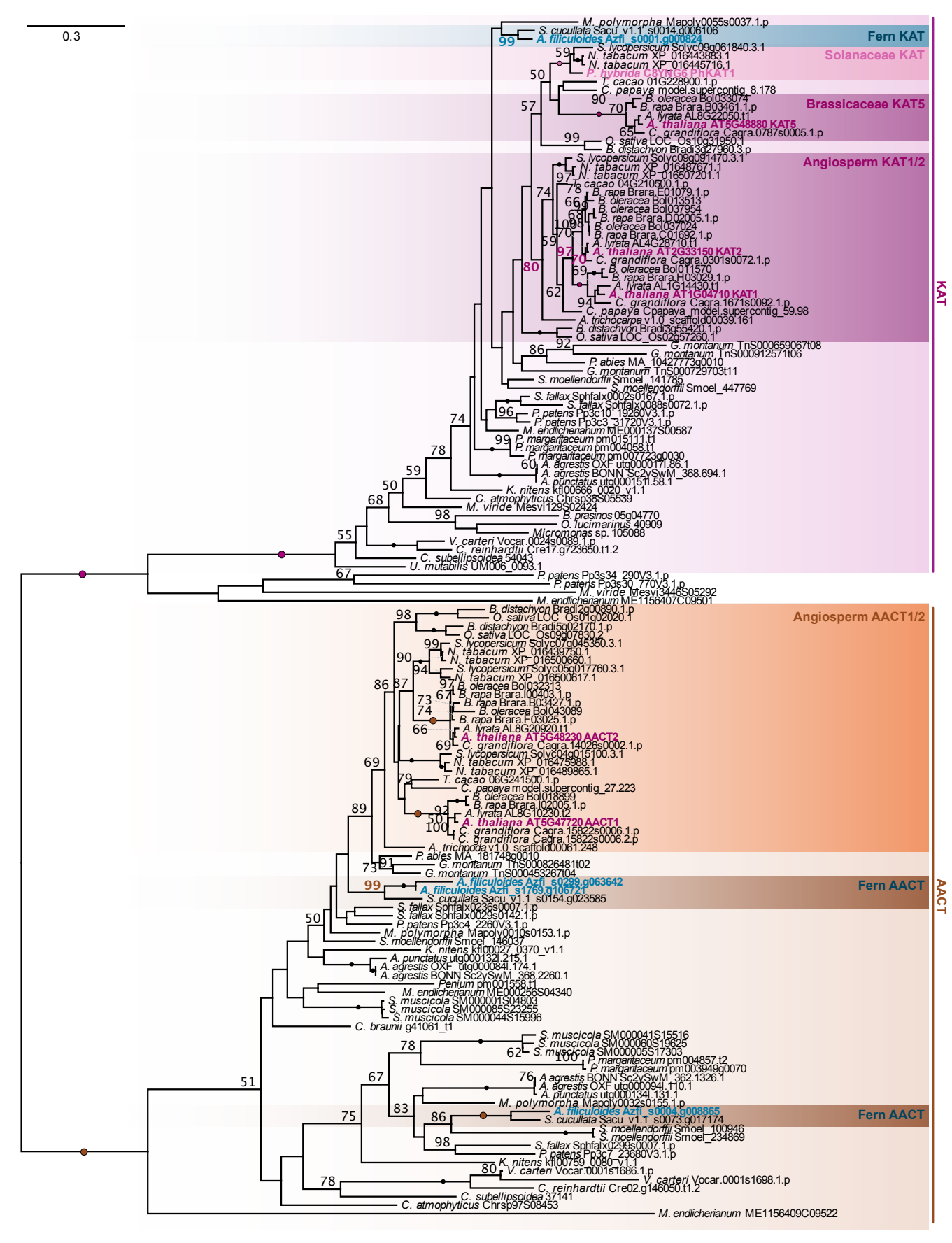
0.3
Fern KAT
Solanaceae KAT
Brassicaceae KAT5
Angiosperm KAT1/2
KAT
Angiosperm AACT1/2
Fern AACT
Fern AACT
AACT
M. polymorpha Mapoly0055s0037.1.p
S. cucullata Sacu_v1.1_s0014.g006106
A. filiculoides Azfi_s0001.g000824
S. lycopersicum Solyc09g061840.3.1
N. tabacum XP_016443883.1
N. tabacum XP_016445716.1
P. hybrida C8YNG6 PhKAT1
T. cacao 01G228900.1.p
C. papaya model.supercontig_8.178
B. oleracea Bol033074
B. rapa Brara.B03461.1.p
A. lyrata AL8G22050.t1
A. thaliana AT5G48880 KAT5
C. grandiflora Cagra.0787s0005.1.p
O. sativa LOC_Os10g31950.1
B. distachyon Bradi3g27960.3.p
S. lycopersicum Solyc09g091470.3.1
N. tabacum XP_016487671.1
N. tabacum XP_016507201.1
T. cacao 04G210500.1.p
B. rapa Brara.E01079.1.p
B. oleracea Bol013513
B. oleracea Bol037954
B. rapa Brara.D02005.1.p
B. oleracea Bol037024
B. rapa Brara.C01692.1.p
A. lyrata AL4G28710.t1
A. thaliana AT2G33150 KAT2
C. grandiflora Cagra.0301s0072.1.p
B. oleracea Bol011570
B. rapa Brara.H03029.1.p
A. lyrata AL1G14430.t1
A. thaliana AT1G04710 KAT1
C. grandiflora Cagra.1671s0092.1.p
C. papaya Cpapaya_model.supercontig_59.98
A. trichocarpa v1.0_scaffold00039.161
B. distachyon Bradi3g55420.1.p
O. sativa LOC_Os02g57260.1
G. montanum TnS00065967t08
G. montanum TnS00091257t06
P. abies MA_10427773g0010
G. montanum TnS00072970 3t11
S. moellendorffii Smoel_141785
S. moellendorffii Smoel_447769
S. fallax Sphfalx0002s0167.1.p
S. fallax Sphfalx0088s0072.1.p
P. patens Pp3c10_19260V3.1.p
P. patens Pp3c3_31720V3.1.p
M. endlicherianum ME000137S00587
P. margaritaceum pm015111.t1
P. margaritaceum pm004058.t1
P. margaritaceum pm007723g0030
A. agrestis OXF utg000017l.86.1
A. agrestis BONN Sc2ySwM_368.694.1
A. punctatus utg000151l.58.1
K. nitens kfl00666_0020_v1.1
C. atmophyticus Chrsp38S05539
M. viride Mesvi129S02424
B. prasinos 05g04770
O. lucimarinus 40909
Micromonas sp. 105088
V. carteri Vocar.0024s0089.1.p
C. reinhardtii Cre17.g723650.t1.2
C. subellipsoidea 54043
U. mutabilis UM006_0093.1
P. patens Pp3s34_290V3.1.p
P. patens Pp3s30_770V3.1.p
M. viride Mesvi3446S05292
M. endlicherianum ME1156407C09501
B. distachyon Bradi2g00890.1.p
O. sativa LOC_Os01g02020.1
B. distachyon Bradi5g02170.1.p
O. sativa LOC_Os09g07830.2
S. lycopersicum Solyc07g045350.3.1
N. tabacum XP_016439750.1
N. tabacum XP_016500660.1
S. lycopersicum Solyc05g017760.3.1
N. tabacum XP_016500617.1
B. oleracea Bol032313
B. rapa Brara.I00403.1.p
B. rapa Brara.B03427.1.p
B. oleracea Bol043089
B. rapa Brara.F03025.1.p
A. lyrata AL8G20920.t1
A. thaliana AT5G48230 AACT2
C. grandiflora Cagra.14026s0002.1.p
S. lycopersicum Solyc04g015100.3.1
N. tabacum XP_016475988.1
N. tabacum XP_016489865.1
T. cacao 06G241500.1.p
C. papaya model.supercontig_27.223
B. oleracea Bol018899
B. rapa Brara.I02005.1.p
A. lyrata AL8G10230.t2
A. thaliana AT5G47720 AACT1
C. grandiflora Cagra.15822s0006.1.p
C. grandiflora Cagra.15822s0006.2.p
A. trichopoda v1.0_scaffold00061.248
P. abies MA_18174g0010
G. montanum TnS000826481t02
G. montanum TnS00045326 7t04
A. filiculoides Azfi_s0299.g063642
A. filiculoides Azfi_s1789.g106721
S. cucullata Sacu_v1.1_s0154.g023585
S. fallax Sphfalx0236s0007.1.p
S. fallax Sphfalx0029s0142.1.p
P. patens Pp3c4_2260V3.1.p
M. polymorpha Mapoly0010s0153.1.p
S. moellendorffii Smoel_146037
K. nitens kfl00027_0370_v1.1
A. punctatus utg000132l.215.1
A. agrestis OXF utg000084l.174.1
A. agrestis BONN Sc2ySwM_368.2260.1
Penium pm001558.t1
M. endlicherianum ME000256S04340
S. muscicola SM000001S04803
S. muscicola SM000085S22255
S. muscicola SM000044S15996
C. braunii g41061_t1
S. muscicola SM000041S15516
S. muscicola SM000060S19625
S. muscicola SM000005S17303
P. margaritaceum pm004857.t2
P. margaritaceum pm003949g0070
A. agrestis BONN Sc2ySwM_362.1326.1
A. agrestis OXF utg000014l.110.1
A. punctatus utg000134l.131.1
M. polymorpha Mapoly0032s0155.1.p
A. filiculoides Azfi_s0004.g008865
S. cucullata Sacu_v1.1_s0073.g017174
S. moellendorffii Smoel_100946
S. moellendorffii Smoel_234869
S. fallax Sphfalx0029s0007.1.p
P. patens Pp3c7_23690V3.1.p
K. nitens kfl00759_0080_v1.1
V. carteri Vocar.0001s1686.1.p
V. carteri Vocar.0001s1698.1.p
C. reinhardtii Cre02.g146050.t1.2
C. subellipsoidea 37141
C. atmophyticus Chrsp97S08453
M. endlicherianum ME1156409C09522

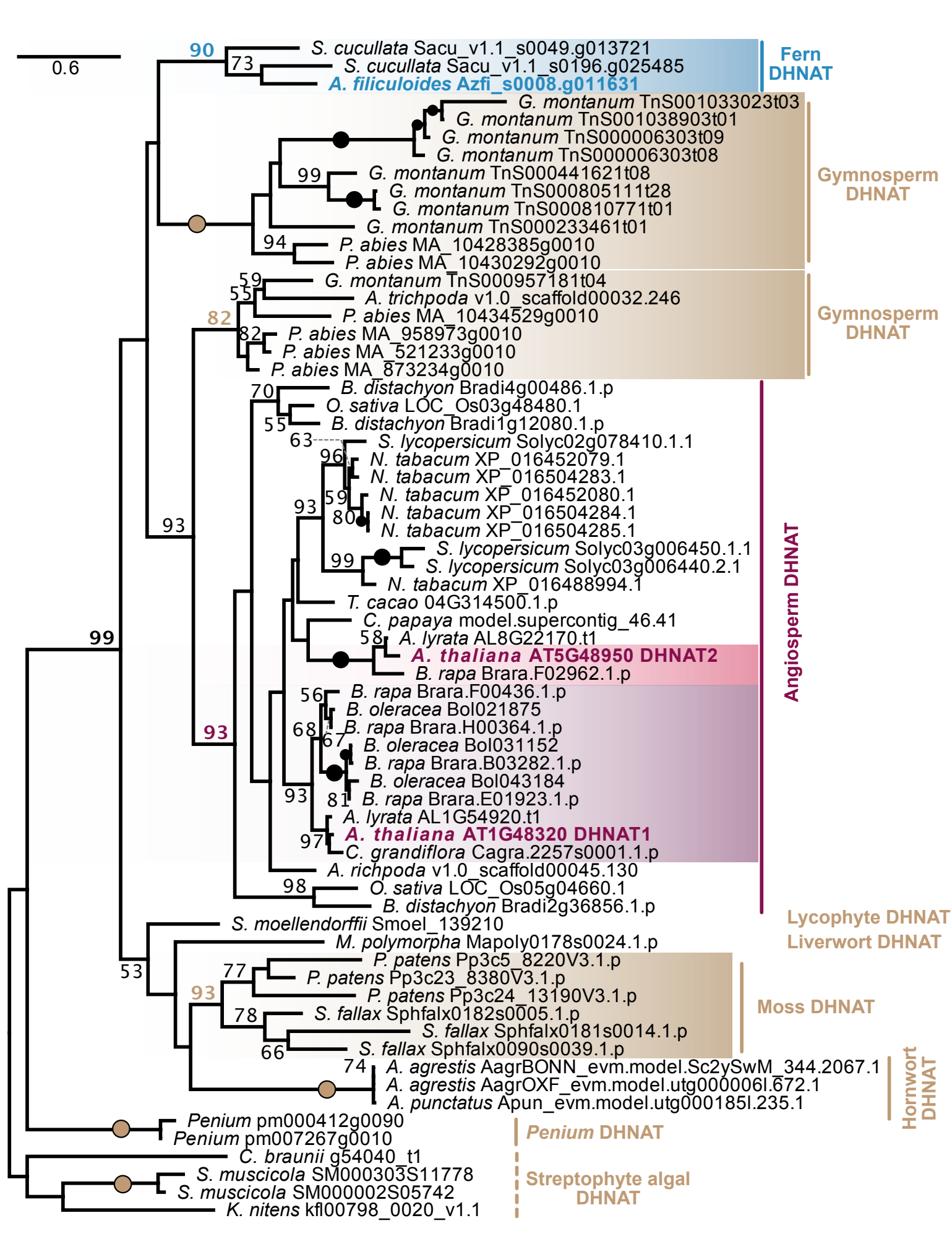
0.6
S. cucullata Sacu_v1.1_s0049.g013721
S. cucullata Sacu_v1.1_s0196.g025485
A. filiculoides Azfi_s0008.g011631
Fern DHNAT
G. montanum TnS001033023t03
G. montanum TnS001038903t01
G. montanum TnS000006303t09
G. montanum TnS000006303t08
G. montanum TnS000441621t08
G. montanum TnS000805111t28
G. montanum TnS000810771t01
G. montanum TnS000233461t01
P. abies MA_10428385g0010
P. abies MA_10430292g0010
Gymnosperm DHNAT
G. montanum TnS000957181t04
A. trichpoda v1.0_scaffold00032.246
P. abies MA_10434529g0010
P. abies MA_958973g0010
P. abies MA_521233g0010
P. abies MA_873234g0010
Gymnosperm DHNAT
B. distachyon Bradi4g00486.1.p
O. sativa LOC_Os03g48480.1
B. distachyon Bradi1g12080.1.p
S. lycopersicum Solyc02g078410.1.1
N. tabacum XP_016452079.1
N. tabacum XP_016504283.1
N. tabacum XP_016452080.1
N. tabacum XP_016504284.1
N. tabacum XP_016504285.1
S. lycopersicum Solyc03g006450.1.1
S. lycopersicum Solyc03g006440.2.1
N. tabacum XP_016488994.1
T. cacao 04G314500.1.p
C. papaya model.supercontig_46.41
A. lyrata AL8G22170.t1
A. thaliana AT5G48950 DHNAT2
B. rapa Brara.F02962.1.p
B. rapa Brara.F00436.1.p
B. oleracea Bol021875
B. rapa Brara.H00364.1.p
B. oleracea Bol031152
B. rapa Brara.B03282.1.p
B. oleracea Bol043184
B. rapa Brara.E01923.1.p
A. lyrata AL1G54920.t1
A. thaliana AT1G48320 DHNAT1
C. grandiflora Cagra.2257s0001.1.p
A. richpoda v1.0_scaffold00045.130
O. sativa LOC_Os05g04660.1
B. distachyon Bradi2g36856.1.p
Angiosperm DHNAT
S. moellendorffii Smoel_139210
M. polymorpha Mapoly0178s0024.1.p
Lycophyte DHNAT
Liverwort DHNAT
P. patens Pp3c5_8220V3.1.p
P. patens Pp3c23_8380V3.1.p
P. patens Pp3c24_13190V3.1.p
S. fallax Sphfalx0182s0005.1.p
S. fallax Sphfalx0181s0014.1.p
S. fallax Sphfalx0090s0039.1.p
Moss DHNAT
A. agrestis AagrBONN_evm.model.Sc2ySwM_344.2067.1
A. agrestis AagrOXF_evm.model.utg000006l.672.1
A. punctatus Apun_evm.model.utg000185l.235.1
Hornwort DHNAT
Penium pm000412g0090
Penium pm007267g0010
Penium DHNAT
C. braunii g54040_t1
S. muscicola SM000303S11778
S. muscicola SM000002S05742
K. nitens kfl00798_0020_v1.1
Streptophyte algal DHNAT

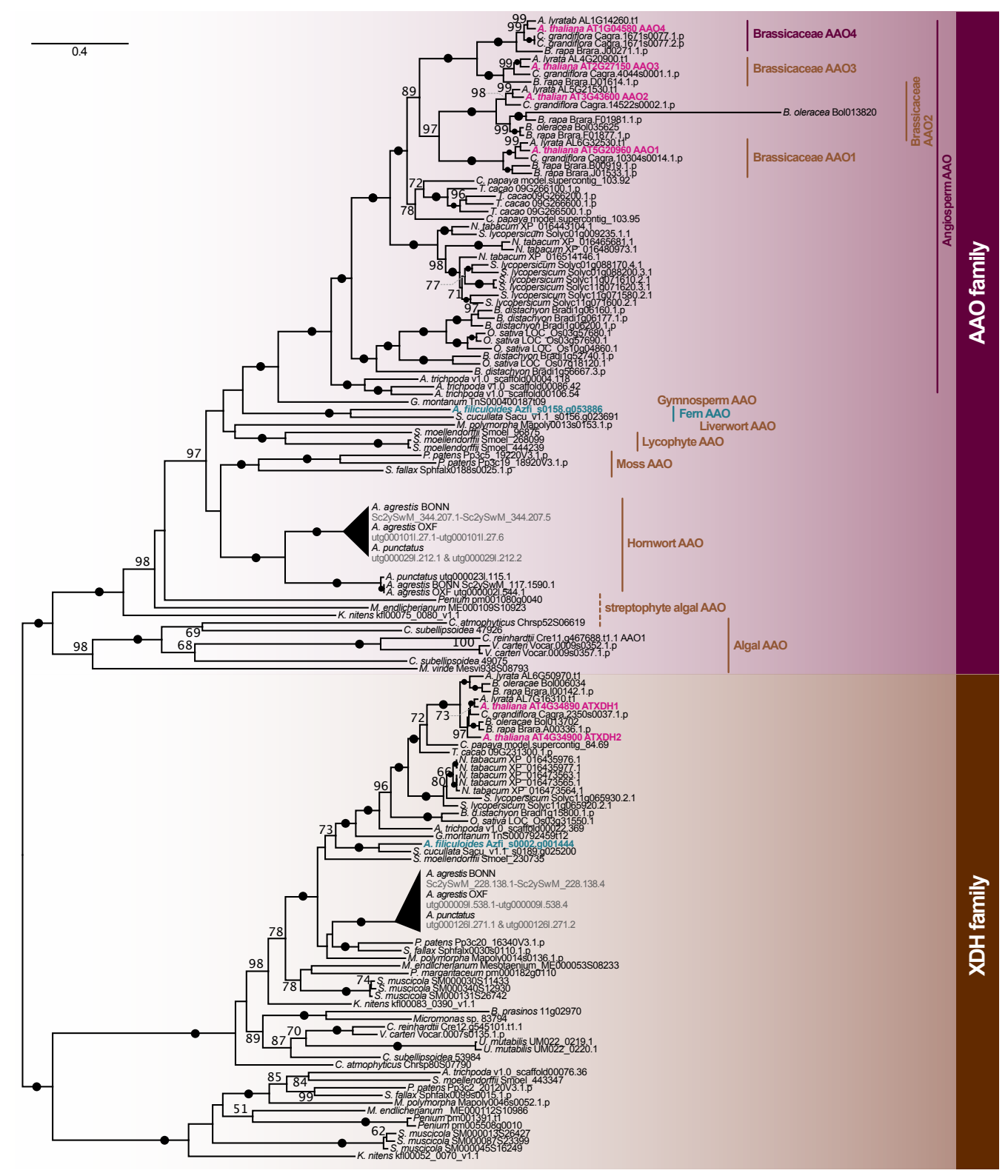
0.4
A. lyrata AL1G14260.t1
A. thaliana AT1G04580 AAO4
C. grandiflora Cagra.1671s0077.1.p
C. grandiflora Cagra.1671s0077.2.p
B. rapa Brara_J00271.1.p
A. lyrata AL4G20900.t1
A. thaliana AT2G27150 AAO3
C. grandiflora Cagra.4044s0001.1.p
B. rapa Brara_D01614.1.p
A. lyrata AL5G42530.t1
A. thalian AT3G43600 AAO2
C. grandiflora Cagra.14522s0002.1.p
B. oleracea Bol013820
B. rapa Brara_F01981.1.p
B. oleracea Bol035625
B. rapa Brara_F01977.1.p
A. lyrata AL6G32530.t1
A. thaliana AT5G20960 AAO1
C. grandiflora Cagra.10304s0014.1.p
B. rapa Brara_B00919.1.p
B. rapa Brara_J01533.1.p
C. papaya model.supercontig_103.92
T. cacao 09G266100.1.p
T. cacao 09G266200.1.p
T. cacao 09G266600.1.p
T. cacao 09G266500.1.p
C. papaya model.supercontig_103.95
N. tabacum XP_016443104.1
S. lycopersicum Solyc01g009235.1.1
N. tabacum XP_016465681.1
N. tabacum XP_016480973.1
N. tabacum XP_016514146.1
S. lycopersicum Solyc01g088170.4.1
S. lycopersicum Solyc01g088200.3.1
S. lycopersicum Solyc11g071810.2.1
S. lycopersicum Solyc11g071620.3.1
S. lycopersicum Solyc11g071580.2.1
S. lycopersicum Solyc11g071600.2.1
B. distachyon Bradi1g05160.1.p
B. distachyon Bradi1g06177.1.p
B. distachyon Bradi1g06200.1.p
O. sativa LOC_Os03g57680.1
O. sativa LOC_Os03g57690.1
O. sativa LOC_Os10g04860.1
B. distachyon Bradi1g52740.1.p
O. sativa LOC_Os07g18120.1
B. distachyon Bradi1g56667.3.p
A. trichpoda v1.0_scaffold00004.118
A. trichpoda v1.0_scaffold00086.42
A. trichpoda v1.0_scaffold00106.54
G. montanum TnS000400187109
A. filiculoides Azfi_s0158.g053886
S. cucullata Sacu_v1.1_s0156.g023691
M. polymorpha Mapoly0013s0153.1.p
S. moellendorffii Smoel_96875
S. moellendorffii Smoel_268099
S. moellendorffii Smoel_444239
P. patens Pp3c5_19220V3.1.p
P. patens Pp3c19_18920V3.1.p
S. fallax Sphfalx0188s0025.1.p
A. agrestis BONN
Sc2ySwM_344.207.1-Sc2ySwM_344.207.5
A. agrestis OXF
utg000101l.27.1-utg000101l.27.6
A. punctatus
utg000029l.212.1 & utg000029l.212.2
A. punctatus utg000023l.115.1
A. agrestis BONN Sc2ySwM_117.1590.1
A. agrestis OXF utg000002l.544.1
Penium pm0010890g0040
M. endlicherianum ME000109S10923
K. nitens kfl00075_0080_v1.1
C. atmophyticus Chrsp52S06619
C. subellipsoidea 47926
C. reinhardtii Cre11.g467688.t1.1 AAO1
V. carteri Vocar.0009s0352.1.p
V. carteri Vocar.0009s0357.1.p
C. subellipsoidea 49075
M. viride Mesvi938S08793
A. lyrata AL6G50970.t1
B. oleracae Bol006034
B. rapa Brara_I00142.1.p
A. lyrata AL7G16310.t1
A. thaliana AT4G34890 ATXDH1
C. grandiflora Cagra.2350s0037.1.p
B. oleracae Bol013702
B. rapa Brara.A00336.1.p
A. thaliana AT4G34900 ATXDH2
C. papaya model.supercontig_84.69
T. cacao 09G231300.1.p
N. tabacum XP_016435976.1
N. tabacum XP_016435977.1
N. tabacum XP_016473563.1
N. tabacum XP_016473565.1
N. tabacum XP_016473564.1
S. lycopersicum Solyc11g065930.2.1
S. lycopersicum Solyc11g065920.2.1
B. distachyon Bradi1g15800.1.p
O. sativa LOC_Os03g31550.1
A. trichpoda v1.0_scaffold00022.369
G. montanum TnS000792459t12
A. filiculoides Azfi_s0002.g001444
S. cucullata Sacu_v1.1_s0189.g025200
S. moellendorffii Smoel_230735
A. agrestis BONN
Sc2ySwM_228.138.1-Sc2ySwM_228.138.4
A. agrestis OXF
utg000009l.538.1-utg000009l.538.4
A. punctatus
utg000126l.271.1 & utg000126l.271.2
P. patens Pp3c20_16340V3.1.p
S. fallax Sphfalx0030s0110.1.p
M. polymorpha Mapoly0014s0136.1.p
M. endlicherianum Mesotaenium_ME000053S08233
P. margaritaceum pm0001820g0110
S. muscicola SM000030S11433
S. muscicola SM000340S12930
S. muscicola SM000131S26742
K. nitens kfl00083_0390_v1.1
B. prasinos 11g02970
Micromonas sp. 83794
C. reinhardtii Cre12.g545101.t1.1
V. carteri Vocar.0007s0135.1.p
U. mutabilis UM022_0219.1
U. mutabilis UM022_0220.1
C. subellipsoidea 53984
C. atmophyticus Chrsp60S07790
A. trichpoda v1.0_scaffold00076.36
S. moellendorffii Smoel_443347
P. patens Pp3c2_20120V3.1.p
S. fallax Sphfalx0099s0015.1.p
M. polymorpha Mapoly0046s0052.1.p
M. endlicherianum ME000112S10986
Penium pm0013911.t1
Penium pm0055080g0010
S. muscicola SM000013S26427
S. muscicola SM000087S25399
S. muscicola SM000045S16249
K. nitens kfl00052_0070_v1.1
Brassicaceae AAO4
Brassicaceae AAO3
Brassicaceae AAO2
Brassicaceae AAO1
Angiosperm AAO
Gymnosperm AAO
Fern AAO
Liverwort AAO
Lycophyte AAO
Moss AAO
Hornwort AAO
streptophyte algal AAO
Algal AAO
AAO family
XDH family

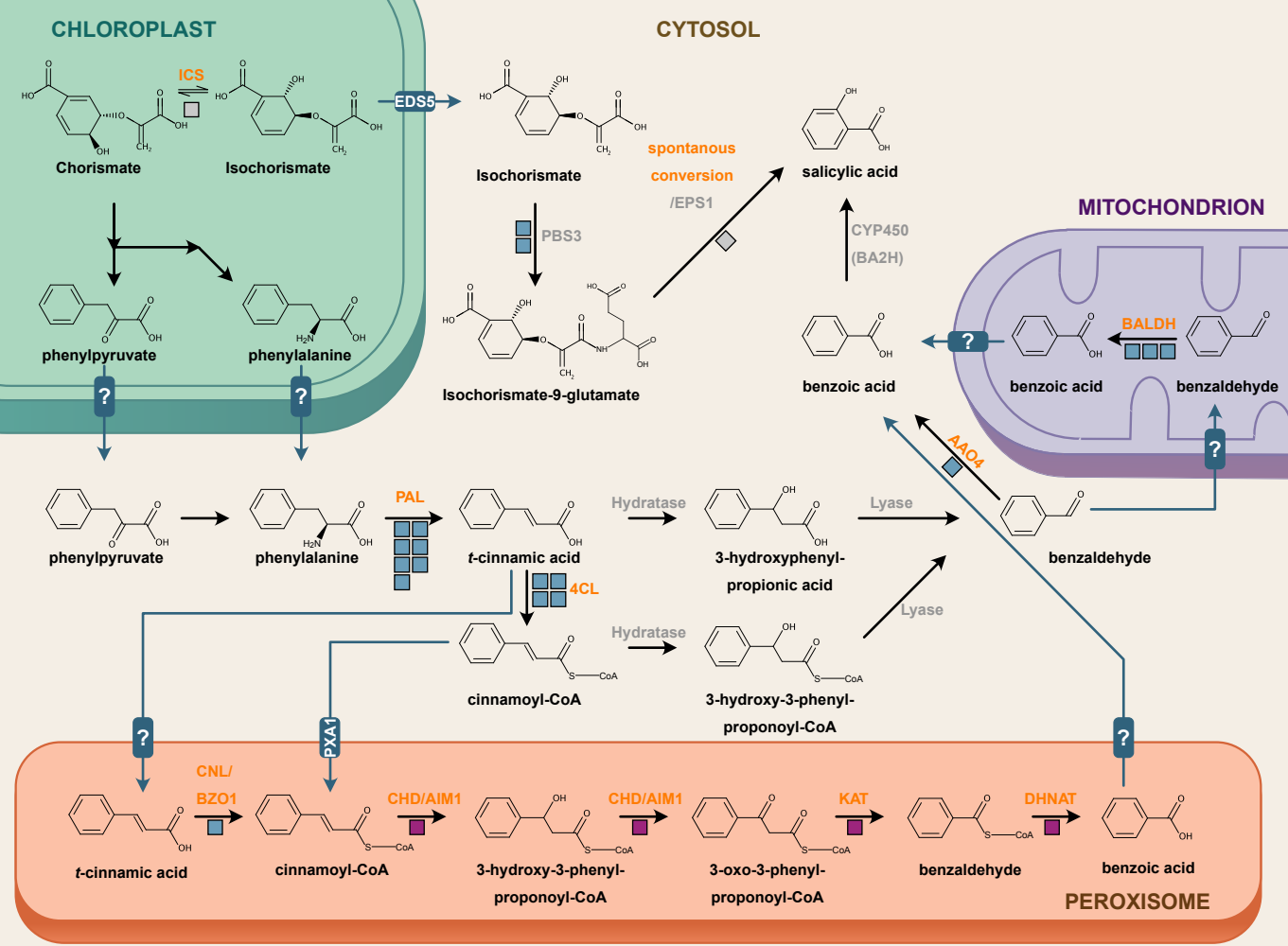
CHLOROPLAST
CYTOSOL
MITOCHONDRION
PEROXISOME
ICS
EDS5
Chorismate
Isochorismate
phenylpyruvate
phenylalanine
PBS3
Isochorismate-9-glutamate
spontanous
conversion
/EPS1
salicylic acid
CYP450
(BA2H)
benzoic acid
BALDH
benzaldehyde
AAO4
PAL
t-cinnamic acid
Hydratase
3-hydroxyphenyl-
propionic acid
Lyase
4CL
cinnamoyl-CoA
3-hydroxy-3-phenyl-
proponoyl-CoA
CNL/
BZO1
PXA1
CHD/AIM1
3-oxo-3-phenyl-
proponoyl-CoA
KAT
DHNAT

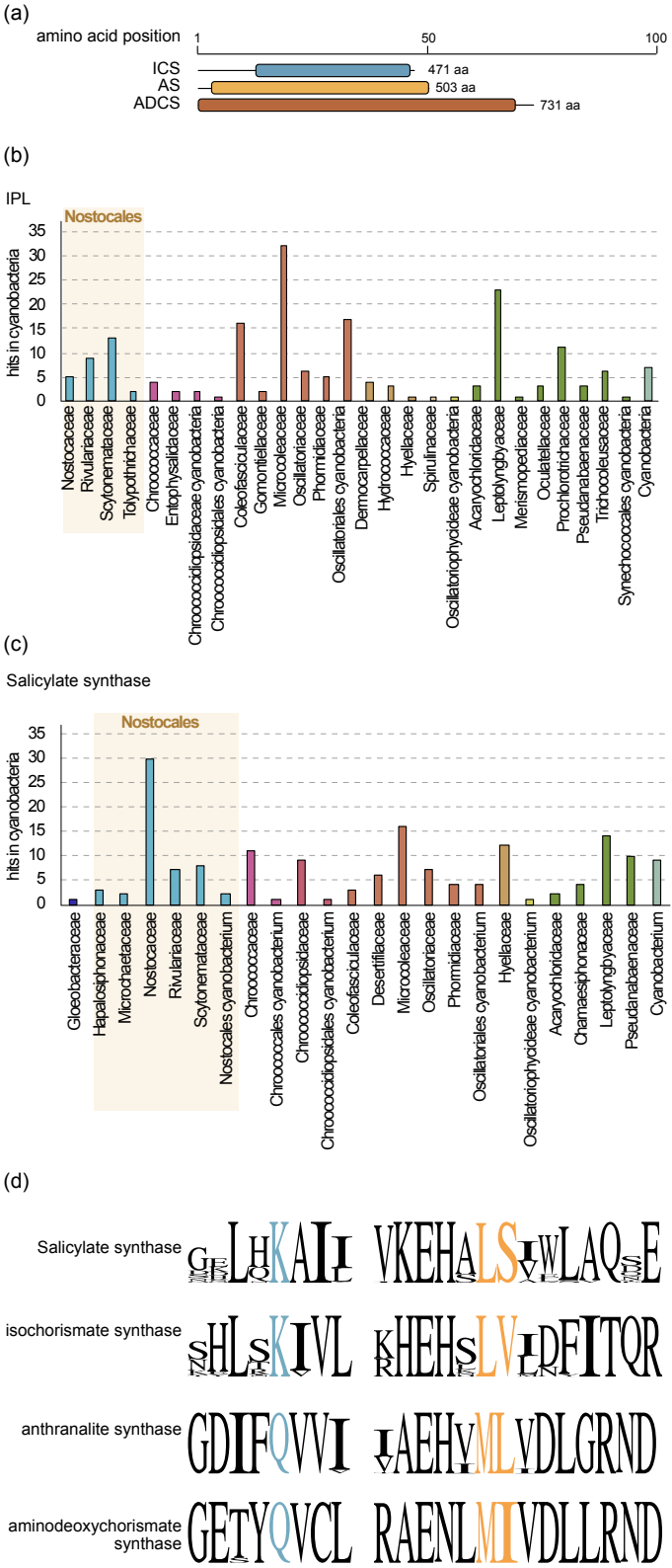
(a)
amino acid position
1
50
100
ICS
471 aa
AS
503 aa
ADCS
731 aa
(b)
IPL
Nostocales
hits in cyanobacteria
0
5
10
15
20
25
30
35
Nostocaceae
Rivulariaceae
Scytonemataceae
Tolypothrichaceae
Chroococcaceae
Entophysalidaceae
Chroococcidiopsidaceae cyanobacteria
Chroococcidiopsidales cyanobacteria
Coleofasciculaceae
Gomontiellaceae
Microcoleaceae
Oscillatoriaceae
Phormidiaceae
Oscillatoriales cyanobacteria
Dermocarpellaceae
Hydrococcaceae
Hyellaceae
Spirulinaceae
Oscillatoriophycideae cyanobacteria
Acaryochloridaceae
Leptolyngbyaceae
Merismopediaceae
Oculatellaceae
Prochlorotrichaceae
Pseudanabaenaceae
Trichocoleusaceae
Synechococcales cyanobacteria
Cyanobacteria
(c)
Salicylate synthase
Nostocales
hits in cyanobacteria
0
5
10
15
20
25
30
35
Gloeobacteraceae
Hapalosiphonaceae
Microchaetaceae
Nostocaceae
Rivulariaceae
Scytonemataceae
Nostocales cyanobacterium
Chroococcaceae
Chroococcales cyanobacterium
Chroococcidiopsidaceae
Chroococcidiopsidales cyanobacterium
Coleofasciculaceae
Desertifilaceae
Microcoleaceae
Oscillatoriaceae
Phormidiaceae
Oscillatoriales cyanobacterium
Hyellaceae
Oscillatoriophycideae cyanobacterium
Acaryochloridaceae
Chamaesiphonaceae
Leptolyngbyaceae
Pseudanabaenaceae
Cyanobacterium
(d)
Salicylate synthase
isochorismate synthase
anthranalite synthase
aminodeoxychorismate synthase

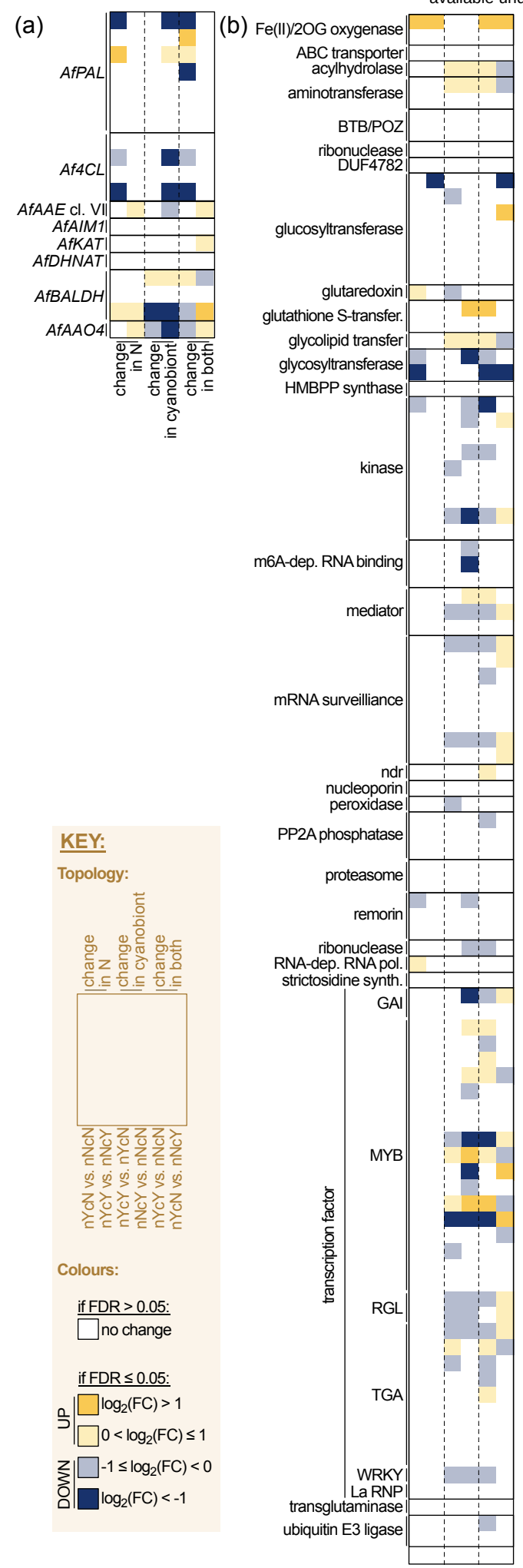
(a)
AfPAL
Af4CL
AfAAE cl. VII
AfAIM1
AfKAT
AfDHNAT
AfBALDH
AfAAO4
change in N
change in cyanobiont
change in both
(b)
Fe(II)/2OG oxygenase
ABC transporter
acylhydrolase
aminotransferase
BTB/POZ
ribonuclease
DUF4782
glucosyltransferase
glutaredoxin
glutathione S-transfer.
glycolipid transfer
glycosyltransferase
HMBPP synthase
kinase
m6A-dep. RNA binding
mediator
mRNA surveilliance
ndr
nucleoporin
peroxidase
PP2A phosphatase
proteasome
remorin
ribonuclease
RNA-dep. RNA pol.
strictosidine synth.
transcription factor
GAI
MYB
RGL
TGA
WRKY
La RNP
transglutaminase
ubiquitin E3 ligase
KEY:
Topology:
change in N
change in cyanobiont
change in both
nYcN vs. nNcN
nYcY vs. nNcY
nYcY vs. nYcN
nNcY vs. nNcN
nYcY vs. nNcN
nYcN vs. nNcY
Colours:
if FDR > 0.05:
no change
if FDR ≤ 0.05:
UP
log2(FC) > 1
0 < log2(FC) ≤ 1
DOWN
-1 ≤ log2(FC) < 0
log2(FC) < -1